Research Square

Preprints are preliminary reports that have not undergone peer review.
They should not be considered conclusive, used to inform clinical practice,
or referenced by the media as validated information.

Exploring Cavity Size–Dependent Control of Host–Guest Interactions in Cyclodextrins: Linking Spectroscopy, Binding Thermodynamics to Release and Biological Function of 4-Aminopyridine

Koushik Baul
North Bengal University
Priyanka Roy
North Bengal University
Subhankar Choudhury
Malda College
Biswanath Karmakar
North Bengal University
Dibakar Ghosh
North Bengal University
Swarnendu Roy
North Bengal University
Sangita Dey
North Bengal University
Anoop Kumar
North Bengal University
Saurav Sarkar
North Bengal University
Gouranga Nandi
North Bengal University
Mahendra Nath Roy
mahendraroy2002@yahoo.co.in
North Bengal University

Research Article

Keywords:

Posted Date: April 22nd, 2026

DOI: https://doi.org/10.21203/rs.3.rs-9390211/v1

License: This work is licensed under a Creative Commons Attribution 4.0 International License.
Read Full License

Additional Declarations: No competing interests reported.

Version of Record: A version of this preprint was published at Journal of Inclusion Phenomena and Macrocyclic Chemistry on June 3rd, 2026. See the published version at https://doi.org/10.1007/s10847-026-01356-x.

Abstract

Cavity size plays a decisive role in governing host–guest interactions in cyclodextrin-based inclusion systems. In this study, the encapsulation behavior of 4-aminopyridine (4-AP) with α- and β-cyclodextrins (α-CD and β-CD) was systematically investigated to elucidate the relationship between cavity dimensions, binding thermodynamics, and functional performance. Inclusion complex formation was confirmed by ^1H NMR, UV–visible, FTIR, fluorescence spectroscopy, and ESI–MS analyses, revealing distinct cavity-dependent binding modes. Pronounced upfield shifts of inner cavity protons (H3 and H5), along with guest proton perturbations, indicated deeper inclusion and stronger stabilization of 4-AP within the β-CD cavity compared to α-CD.

Thermodynamic parameters demonstrated enhanced binding affinity and stability for the β-CD complex, consistent with its optimal cavity size. Density functional theory (DFT) calculations further corroborated the experimental findings, providing insights into inclusion geometry, interaction energies, and non-covalent stabilization, while reduced density gradient (RDG) analysis confirmed the dominance of van der Waals and hydrogen bonding interactions. In vitro release studies revealed a cavity size–dependent modulation of drug release, with β-CD complexes exhibiting more sustained release profiles relative to α-CD and free 4-AP, indicating improved encapsulation efficiency and controlled delivery behavior.

Importantly, biological evaluations demonstrated that cyclodextrin inclusion significantly influences functional activity. Antioxidant and antimicrobial assays showed enhanced activity for the inclusion complexes, particularly for β-CD, compared to the free drug, highlighting the role of improved stability and molecular dispersion. Furthermore, in vitro cytotoxicity studies using A549 human lung adenocarcinoma cells confirmed that β-CD encapsulation leads to superior biological response, attributable to optimized release and stronger host–guest interactions.

Overall, this study establishes a direct correlation between cyclodextrin cavity size, binding energetics, release behavior, and biological function, demonstrating that cavity size–dependent control of host–guest interactions can be strategically exploited to enhance drug performance.

1. Introduction

The stabilization and modulation of small bioactive molecules through supramolecular encapsulation remain central themes in host–guest chemistry. Cyclodextrins (CDs), cyclic oligosaccharides composed of α-(1→4) linked D-glucopyranose units, possess a hydrophobic internal cavity and hydrophilic exterior, enabling the inclusion of suitably sized guest molecules in aqueous media.[1–3] Their ability to enhance aqueous solubility, chemical stability, and bioavailability has led to widespread pharmaceutical applications.[4, 5]

Among the native cyclodextrins, α-cyclodextrin (α-CD) and β-cyclodextrin (β-CD) differ significantly in cavity diameter (≈ 4.7–5.3 Å for α-CD and ≈ 6.0–6.5 Å for β-CD) (Scheme 1), which directly influences guest selectivity, orientation, and thermodynamic stability.[6, 7] Subtle variations in cavity dimensions

can alter the balance between hydrophobic interactions, hydrogen bonding, van der Waals forces, and desolvation energetics, ultimately dictating the formation constant and structural organization of the inclusion complex.[8]

4-Aminopyridine (4-AP), a heteroaromatic amine widely employed as a potassium channel blocker in neurological disorders, exhibits moderate aqueous solubility and a planar aromatic framework that renders it an ideal probe for cavity-size-dependent inclusion phenomena.[9, 10] Previous investigations have demonstrated the formation of inclusion complexes between 4-AP and α-cyclodextrin, highlighting the role of steric complementarity and hydrogen bonding in complex stabilization.[11] However, to the best of our knowledge, a comprehensive comparative evaluation of 4-AP inclusion within α- and β-cyclodextrins—combining spectroscopic characterization, quantitative determination of association constants and phase solubility behavior, in vitro biological assessment, drug release profiling, and density functional theory (DFT) analysis—has not yet been systematically reported.

Given the marked difference in cavity dimensions between α-CD and β-CD, it is anticipated that β-CD may provide distinct binding geometry, altered inclusion depth, and modified stabilization energy relative to α-CD. From a supramolecular design perspective, understanding how cavity expansion affects host–guest energetics is essential for rational selection of cyclodextrins in drug delivery applications.

In this context, the present work presents a detailed comparative study of the inclusion behavior of 4-aminopyridine with α- and β-cyclodextrins. Complex formation and structural features were established through ^1H NMR, FT-IR, and UV–VIS spectroscopy, while association constants were employed to quantify binding affinity. The impact of encapsulation on antioxidant and antimicrobial activity, cytotoxicity, and in vitro drug release was systematically evaluated to assess functional modulation upon complexation. Complementary density functional theory (DFT) calculations were performed to optimize host–guest geometries and estimate binding energies. Correlation of experimental thermodynamic parameters with theoretical stabilization energies enables deeper insight into cavity-size-dependent host–guest interactions and supports the development of structure–stability–function relationships relevant to supramolecular drug delivery systems.

2. Experimental section

2.1. Materials

4-Aminopyridine (4-AP, ≥ 98%) was purchased from Sisco Research Laboratories Pvt. Ltd., India. α-Cyclodextrin (α-CD, ≥ 99%) was obtained from TCI Chemicals India Pvt. Ltd. and used without further purification. β-Cyclodextrin (β-CD; purity > 97.0%) was sourced from Sigma-Aldrich, India (Table S1). Double-distilled water was used throughout all experiments. Disodium hydrogen phosphate was purchased from Rankem, India, sodium chloride from SRL, India, and potassium dihydrogen phosphate from Emplura. Dialysis membrane-60 was obtained from HiMedia, India. The human lung adenocarcinoma (A549) cell line was obtained from the National Centre for Cell Science (NCCS), Pune,

India. Sodium bicarbonate, Minimum Essential Medium Eagle (MEM) media, cell culture tested PBS, 10× Trypsin EDTA solution were purchased from HiMedia, India. MTT [3-(4,5-dimethylthiazol-2-yl)-2,5 diphenyl tetrazolium bromide] dye was purchased from Bio Basic Canada Inc., Canada. Isopropanol, cell culture plates were purchased from Merck, India and Tarsons, India, respectively.

2.2. Methods

All chemicals and samples were precisely measured at 298.15 K using a METTLER TOLEDO AG-285 analytical balance, ensuring an accuracy of ± 0.01 mg. During spectral measurements, the temperature of the samples was maintained at a constant value by an automated digital thermostatic control unit, providing stable and controlled experimental conditions. The 1H NMR data were meticulously charted utilizing the advanced capabilities of the Mestrenova software. Notably, all spectroscopic experiments were conducted in water solution

2.3 UV–visible spectroscopy

UV–visible titration experiments for comparing 4-AP inclusion complexes with α-CD and β-CD were conducted using an Agilent 8453 spectrophotometer. The temperature for accurate determination of the association constants was maintained with a digital thermostatic system. All absorption measurements were performed under strictly controlled conditions at 293 ± 0.15 K.

2.4. 1H NMR spectroscopy

All NMR spectra were recorded by Bruker Avi HD-300 spectrometer at 300 MHz and 25 ºC in D_2O

2.5 FT-IR Spectroscopy

FT-IR spectra of the samples were recorded on an Agilent Cary 630 FTIR spectrometer using the conventional KBr pellet technique. For analysis, pellets were prepared by homogeneously mixing approximately 1 mg of the solid inclusion complex (4-AP with α-CD or β-CD) with 100 mg of spectroscopic-grade KBr. The measurements were then carried out in the wavenumber range of 4000–450 cm^{-1} under ambient conditions to obtain the infrared spectral profiles.

2.6. Antioxidant activities assay

DPPH Scavenging Activity

The free radical scavenging activity of 4-AP, 4-AP-αCD, and 4-AP-βCD samples was measured through the DPPH (2,2-diphenylpicrylhydrazyl) scavenging assay, according to the method of Blois (1958). Briefly, 100 µL of 1 mg/mL of each sample solution was mixed with 2.9 mL of 0.1 mM methanolic DPPH solution and incubated in the dark at RT for 30 min, and the absorbance was measured at 517 nm.

$ABTS^{+}$ Scavenging Activity

The ABTS (2,2'-azino-bis (3-ethylbenzothiazoline-6-sulphonic acid) scavenging activity was performed according to the method of Re et al. (1999). Briefly, 7 mM ABTS solution was prepared in the aqueous

solution of potassium persulphate (2.45 mM) for the generation of ABTS radical cation ($ABTS^{+}$). Then, dilution of the solution was done with ethanol till the absorbance reached 0.70 ± 0.05 at 734 nm. This solution was then incubated in the dark for 12 hours, after which 2 mL of this $ABTS^{+}$ solution was mixed with 100 µL of each sample solution. This reaction mixture was then allowed to rest for a few minutes, and then the absorbance was taken at 734 nm.

Superoxide Scavenging Activity

The evaluation of superoxide radical scavenging activity for the synthesized samples was conducted following the methodology outlined by Moein et al. (2008). The reaction mixture comprised 1 mL of the sample under investigation, 1 mL of 312 µM NBT solution, 1 mL of 936 µM NADH solution, and 10 µL of 120 µM PMS. The light-induced response was carried out under fluorescent lamps, with the radical scavenging activity measured at a wavelength of 560 nm.

The percentage scavenging activity of each parameter was calculated from the equation below:

Scavenging effect (%) = 100 × (Ao - As)/Ao

Where Ao is the absorbance of the blank and As is the absorbance of the sample.

2.7 Antioxidant activity assay

To perform the antimicrobial activity of the samples, two Gram-negative bacteria, such as *Bacillus megaterium* ATCC 14581 and *Staphylococcus aureus* ATCC 11632, and two Gram-positive bacteria, such as *Salmonella typhimurium* ATCC 25241 *and Escherichia coli* ATCC 11229, were used. 100 µL of the pure culture was spread with an L-spreader on nutrient media (solidified in petri plates). After that, blotting paper discs (0.5 cm diameter) dipped separately in 4-AP, 4-AP-αCD, and 4-AP-βCD sample solutions were placed on each of the petri plates and sealed with parafilm [12]. After incubation at 34°C for 24 hours, the pictures of inhibition zones were taken.

2.7 In Vitro Release Study

The in vitro release behavior of the 4-AP inclusion complexes with both α-cyclodextrin and β-cyclodextrin was investigated using a vertical Franz diffusion cell apparatus. The receptor compartment was filled with sodium phosphate buffer solution (pH 7.4), and the system temperature was maintained at 37 ± 0.5°C to mimic physiological conditions throughout the experiment[13]. A pre-soaked dialysis membrane was fixed between the donor and receptor compartments, and the respective inclusion complex (4-AP–α-CD or 4-AP–β-CD) was uniformly placed in the donor chamber.

At predetermined intervals (1, 2, 3, 4, and 5 h), 1 mL aliquots were withdrawn from the receptor compartment and immediately replaced with an equal volume of fresh buffer to preserve constant volume and sink conditions. The amount of 4-AP released from each complex was quantified using UV–Visible spectrophotometry. The cumulative percentage release of 4-AP from both α-CD and β-CD

inclusion systems at each time point is presented in Table S8 and S9, enabling comparative evaluation of their release profiles.

2.8 Cell Culture:

Human lung adenocarcinoma (A549) cell line was cultured in MEM media supplemented with 10% FCS (Foetal Calf Serum), 1% Penicillin-Streptomycin antibiotic and 2.2 g/L of Sodium bicarbonate in 100 mm cell culture plates at 37°C, 5% CO_2 incubator. Cells were passaged on appropriate (80–90%) confluency.

2.9 Cell Viability Assay (MTT Assay):

On a 96 well microtiter plate, approximately 100 µL media containing cells were seeded at a density of 5×10^3 cells per well and kept it for overnight at 37°C, 5% CO_2 incubator. Next day, 4-AP, IC and its complexes were added in a triplicate manner at concentrations of 50, 100, 150, 200 and 250 µg/mL and kept it again for overnight incubation under same condition. The day after treatment, media was replaced by 10 µL of MTT dye [Stock solution 5 mg/mL, dissolved in 1× PBS] solution and kept it again for 3 h at 37°C, 5% CO_2 incubator. After 3 h, 50 µL of isopropanol was added to each well to solubilize the purple formazan crystals and the plate was gently shaken for 5 min. An absorbance was measured at 620 nm. The Percentage of Cytotoxicity was calculated as, Percentage of Cytotoxicity (%) = [{(Y – X)/Y} ×100], where, Y is the mean OD of Blank and X is the mean OD of cells treated with drugs [14, 15].

2.8 Computational details

All quantum chemical calculations were performed using Density Functional Theory (DFT) as implemented in *Gaussian 16* [16]. Ground-state geometries of 4-aminopyridine (4-AP), α-cyclodextrin (α-CD), β-cyclodextrin (β-CD), and their corresponding 1:1 inclusion complexes (4-AP-α-CD and 4-AP-β-CD) were fully optimized at the B3LYP/6–31 + G(d) level of theory. The hybrid B3LYP functional, augmented with dispersion correction, was employed to ensure reliable treatment of non-covalent interactions governing host–guest stabilization, including hydrogen bonding, dispersion forces, and possible π-driven interactions.[17]

To approximate experimental aqueous conditions, solvent effects were incorporated using the Polarizable Continuum Model (PCM) with the integral equation formalism variant (IEF-PCM) during geometry optimization [18, 19]. Harmonic vibrational frequency analyses were performed at the same level of theory to verify that all optimized structures correspond to true minima on the potential energy surface (no imaginary frequencies).

The nature and spatial distribution of weak intermolecular interactions were examined using the Non-Covalent Interaction (NCI) index based on reduced density gradient (RDG) analysis [20, 21]. RDG isosurfaces and sign(λ_2)ρ plots were generated using the Multiwfn 3.7 program to distinguish hydrogen bonding, van der Waals contacts, and steric repulsion within the inclusion cavity.[22]

To probe electronic redistribution upon encapsulation, molecular electrostatic potential (MESP) maps and charge density distributions were computed at the same theoretical level. These analyses provide

insight into host–guest complementarity and possible charge-transfer contributions to complex stabilization.

The adsorption (binding) energy (ΔE_ads) of each inclusion complex was calculated according to:

$\Delta E_{ads} = E_{IC} - E_{4\text{-}AP} - E_{CD}$ where E_{IC} represents the total energy of the optimized inclusion complex (4-AP–α-CD or 4-AP–β-CD), E_{4-AP} corresponds to the energy of the isolated 4-AP molecule, and E_{CD} denotes the energy of the respective isolated cyclodextrin (α-CD or β-CD).. More negative ΔE_{ads} values indicate stronger thermodynamic stabilization of the inclusion complex.

3. Result and Discussions

The guest molecule investigated in this study, 4-aminopyridine (4-AP), exhibits moderate aqueous solubility and contains a heteroaromatic pyridine ring substituted with an amino group capable of hydrogen bonding and dipolar interactions. The primary objective of this work was to comparatively investigate the inclusion behavior of 4-AP with α-cyclodextrin (α-CD) and β-cyclodextrin (β-CD), focusing on binding stoichiometry, interaction mechanisms, and thermodynamic stabilization.

All solution-phase studies were carried out in aqueous medium at ambient temperature. Host–guest complex formation was initially monitored by UV–visible absorption spectroscopy, where progressive spectral changes upon addition of cyclodextrin confirmed interaction. The stoichiometry of complexation was determined using Job's method of continuous variation, establishing a predominant 1:1 host–guest binding mode for both α-CD and β-CD systems. Binding constants (K) were calculated using the Benesi–Hildebrand method, enabling quantitative comparison of the inclusion efficiency of the two cyclodextrins.

Thermodynamic parameters (ΔG°, ΔH°, and ΔS°) were evaluated to elucidate the driving forces governing encapsulation. Analysis of these parameters allowed differentiation between enthalpy-driven stabilization arising from hydrogen bonding and van der Waals interactions, and entropy contributions associated with desolvation and hydrophobic effects. Comparative assessment highlights the influence of cavity size on stabilization, where the larger β-CD cavity is expected to accommodate the aromatic framework of 4-AP more effectively than α-CD.

The solid inclusion complexes were further characterized using FTIR spectroscopy to identify vibrational perturbations indicative of hydrogen-bond reorganization upon encapsulation. In addition, ^1H NMR spectroscopy provided direct evidence of inclusion through upfield shifts of the inner cavity protons (H-3 and H-5) of cyclodextrin and corresponding perturbations in the aromatic proton signals of 4-AP, confirming guest insertion within the hydrophobic cavity.

Collectively, the combined spectroscopic and thermodynamic analyses establish a structure–stability relationship between 4-AP and the two cyclodextrin hosts, enabling a mechanistic comparison of α-CD and β-CD encapsulation efficiency.

3.1. Job’s plot: Determination of stoichiometry behaviour of cyclodextrins

inclusion complex with 4-AP.

The stoichiometry of the 4-aminopyridine (4-AP) inclusion complexes with α-cyclodextrin (α-CD) and β-cyclodextrin (β-CD) was determined using Job’s method of continuous variation[23]. A series of solutions was prepared for each host system in which the total molar concentration of 4-AP and cyclodextrin was kept constant, while the mole fraction of 4-AP was varied from 0 to 1. The mole fraction (R) was defined as $R = \frac{[4\text{-}AP]}{[4\text{-}AP]+[CD]}$.

UV–visible absorption spectra were recorded at 298.15 K, and absorbance changes were monitored at the characteristic λ_max of 4-AP. Job’s plots were constructed by plotting ΔA × R versus R, where ΔA represents the difference in absorbance of 4-AP in the absence and presence of cyclodextrin.

For both α-CD and β-CD systems, the plots exhibited a clear maximum at R ≈ 0.50, indicating the formation of predominant 1:1 (guest:host) inclusion complexes (Fig. 1) Maxima at R ≈ 0.33, 0.50, and 0.66 correspond to 1:2, 1:1, and 2:1 stoichiometries, respectively. The observed 1:1 binding mode is consistent with the model used in subsequent binding-constant calculations and supports a single-guest encapsulation mechanism within the cyclodextrin cavity.(Table S2 and S3).The 1:1 stoichiometry observed from Job’s analysis is structurally rationalized by the geometric complementarity between the single aromatic core of 4-aminopyridine and the hydrophobic cavity of α- and β-cyclodextrins. The molecular dimensions of 4-AP permit efficient encapsulation of one guest molecule per host without steric congestion, while the absence of bulky substituents or multiple hydrophobic domains precludes higher-order complexation. Encapsulation is further stabilized by hydrogen bonding between the amino substituent and cyclodextrin rim hydroxyl groups, together with favorable desolvation effects, rendering the 1:1 complex thermodynamically optimal.

3.2. Determination of binding constant of inclusion complexes in aqueous ethanol by UV–VIS spectroscopy.

UV–visible spectroscopy was employed to investigate the host–guest interactions of 4-aminopyridine (4-AP) with α-cyclodextrin (α-CD) and β-cyclodextrin (β-CD) and to determine their respective association constants using the Benesi–Hildebrand method. Incremental addition of each cyclodextrin to a fixed concentration of 4-AP resulted in systematic changes in absorbance intensity at the characteristic λ_max of 4-AP (Table S4 and S5), indicating inclusion complex formation in aqueous medium at 298.15 K.

The observed spectral variations arise from changes in the microenvironment surrounding 4-AP upon encapsulation within the hydrophobic cavity of the cyclodextrins, leading to modification of the molar

absorptivity (ε). Assuming a 1:1 host–guest binding model, the association constants (Ka) were calculated using the Benesi–Hildebrand double reciprocal equation:

$$\frac{1}{\Delta A} = \frac{1}{\Delta \epsilon \ [4\text{-}AP]\, K_a\, [CD]} + \frac{1}{\Delta \epsilon \ [4\text{-}AP]}$$

1

……

where ΔA represents the absorbance difference of 4-AP in the absence and presence of cyclodextrin, and [CD] refers to either α-CD or β-CD.

In the Benesi–Hildebrand analysis, ΔA represents the change in absorbance of 4-aminopyridine (4-AP) upon addition of cyclodextrin relative to the free guest, while [4-AP] denotes its initial molar concentration. The association constants (Ka) for the inclusion complexes were extracted from the slope and intercept of the corresponding double reciprocal plots constructed according to Eq. 1.[24]

For the 4-AP + α-CD system, the calculated Ka at 298.15 K was 1.35 × 10³ M⁻¹. The excellent linearity of the double reciprocal plot (R^2 = 0.99883) confirms the validity of the assumed 1:1 binding model and is consistent with the stoichiometry obtained from Job's analysis. (Fig. 2) [25, 26]

Under identical experimental conditions, the 4-AP + β-CD complex exhibited a higher association constant of 3.39 × 10³ M⁻¹. Notably, this value is approximately 2.5-fold greater than that of the α-CD system (3.39/1.35 ≈ 2.51), quantitatively demonstrating the superior binding affinity of β-CD toward 4-AP. This enhancement reflects improved cavity–guest complementarity and reduced steric constraints within the larger β-CD cavity.

The standard Gibbs free energy changes (ΔG°) were calculated using:

$$\Delta G^{\circ} = -RT\ln K_a$$

The ΔG° values were determined to be − 4.27 kcal mol⁻¹ for the α-CD complex and − 4.84 kcal mol⁻¹ for the β-CD complex.(Table 1) The negative values confirm spontaneous inclusion in aqueous medium, while the more negative ΔG° for the β-CD complex further substantiates its enhanced thermodynamic stability. This increased stabilization likely arises from more favorable hydrophobic encapsulation of the aromatic pyridine ring, supported by hydrogen bonding and van der Waals interactions within the β-CD cavity.

Table 1
Stability Constant (Ka and ln Ka) and Gibbs Free Energy Change (ΔG) at 298.15 K for the Inclusion Complexation of 4-AP with α-CD & β-CD (1 kcal = 4.2 kJ)

HOST	GUEST	$K_a(M^{-1})$	ln $K_a(M^{-1})$	ΔG°(kcal mol^{-1})
α-CD	4-AP	1.35×10^3	7.20	-4.27
β-CD	4-AP	3.39×10^3	8.12	-4.84

3.3 ^{1}H-NMR Spectroscopy

The inclusion behavior of 4-aminopyridine with α-cyclodextrin and β-cyclodextrin was investigated by ^1H NMR spectroscopy to elucidate the effect of cavity size on host–guest interactions.

In the β-cyclodextrin system, significant upfield shifts (Table S6) were observed for the inner cavity protons H3 (Δδ = −0.10 ppm) and H5 (Δδ = −0.06 ppm), confirming effective inclusion of the guest molecule within the hydrophobic cavity (Fig. 3). In contrast, the aromatic protons of 4-aminopyridine exhibited slight downfield shifts (Δδ = +0.03–0.11 ppm), which can be attributed to deshielding effects arising from hydrogen bonding interactions between the amino group of the guest and the hydroxyl groups at the cyclodextrin rim, as well as partial exposure of the pyridine ring to the polar environment. These observations suggest a preferential orientation in which the aromatic ring is partially embedded within the cavity while the polar functional group remains near the rim.

In comparison, the α-cyclodextrin complex exhibited relatively smaller upfield shifts (Table S7) for the H3 (Δδ = −0.05 ppm) and H5 (Δδ = −0.02 ppm) protons (Fig. 4), indicating weaker or more superficial inclusion due to the smaller cavity. Notably, the aromatic protons of 4-aminopyridine in this system showed a very slight upfield shift (Δδ ≈ −0.01 ppm), consistent with increased shielding in a constrained hydrophobic environment and reduced contribution from hydrogen-bonding interactions.

Overall, the contrasting chemical shift trends between the two systems highlight the critical role of cavity size in governing the inclusion mode. While β-cyclodextrin facilitates deeper inclusion accompanied by significant host–guest interactions at the rim, α-cyclodextrin promotes a more restricted and shallow association. These findings demonstrate that the balance between hydrophobic shielding and hydrogen bonding interactions dictates the observed NMR behavior and provides clear evidence for cavity-dependent inclusion geometry. The larger magnitude of Δδ for β-cyclodextrin compared to α-cyclodextrin further indicates stronger host–guest interaction and greater depth of inclusion.

3.4 FT-IR Spectroscopy:

Fourier-transform infrared (FT-IR) spectroscopy was employed to substantiate the encapsulation of 4-aminopyridine (4-AP) within the α-cyclodextrin cavity. Complex formation is typically reflected through shifts in band position, changes in intensity, peak broadening, or attenuation arising from intermolecular interactions such as hydrogen bonding and spatial confinement.

In the spectrum of α-CD, the broad O–H stretching band appears around 3400 cm^{-1}, while the C–H stretching and bending vibrations are observed near 2924 and 1405 cm^{-1}, respectively. The glycosidic C–O–C stretching band is detected at approximately 1153 cm^{-1}. For 4-AP, characteristic absorptions include N–H stretching of the $–NH_2$ group (~ 3433 cm^{-1}), aromatic C = C stretching (~ 1646 cm^{-1}), C = N and C–N vibrations (around 1593 and 1331 cm^{-1}), and out-of-plane aromatic C–H bending near 817 cm^{-1}.(Fig. 5)

Upon complexation, notable spectral modifications are observed. The O–H stretching band of α-CD shifts to lower frequency (~ 3330 cm^{-1}), indicating hydrogen bond formation. Minor displacements in C–H stretching and bending bands further suggest close host–guest proximity. The N–H stretching band of 4-AP decreases in intensity and shifts toward lower wavenumber (~ 3325 cm^{-1}), supporting hydrogen bonding within the cavity (Fig. 5). The aromatic C = C and related pyridine vibrations also undergo measurable shifts, consistent with reduced vibrational freedom due to encapsulation. Slight variations in the C–O–C region additionally imply interaction at the glycosidic framework.Overall, the collective band shifts and intensity changes confirm that 4-AP is accommodated within the α-CD cavity, most plausibly entering from the pyridine end to establish a stable inclusion complex.

On the other hand, in the spectrum of β-CD, the broad O–H stretching vibration appears around 3371 cm^{-1}, accompanied by C–H stretching bands near 2919 – 2856 cm^{-1}. The H–O–H bending mode is observed around 1630 cm^{-1}, while the glycosidic C–O–C stretching vibration is detected near 1145 cm^{-1}. For 4-AP, prominent absorptions include the N–H stretching of the amine group in the 3300–3400 cm^{-1} region, aromatic C = C stretching around 1645 cm^{-1}, C = N/C–N vibrations in the 1300–1600 cm^{-1} range, and out-of-plane aromatic C–H bending near 820 cm^{-1}.(Fig. 6)

After complex formation, noticeable spectral modifications occur. The O–H stretching band of β-CD shifts toward lower frequency (≈ 3249 cm^{-1}), indicating hydrogen bond involvement. The C–H stretching region shows slight displacement (≈ 2918 cm^{-1}), suggesting close host–guest proximity. The characteristic aromatic C = C band of 4-AP shifts to approximately 1648 cm^{-1}, while the C–N/C = N vibrations move to around 1333 and 1610 cm^{-1}. Additionally, the aromatic C–H bending band shifts to ~ 822–846 cm^{-1}. Minor variations in the C–O–C region (≈ 1151 cm^{-1}) further support structural perturbation of the β-CD framework upon encapsulation. (Fig. 6)

Collectively, the systematic shifts and intensity changes confirm that 4-AP is accommodated within the β-CD cavity, with the pyridine moiety likely penetrating the hydrophobic interior to establish a stable inclusion complex.

3.5 Antioxidant activity assay

The antioxidant activity was evaluated using DPPH, $ABTS^+$, and superoxide scavenging assays, in which 4-AP-βCD showed the best results, followed by 4-AP-αCD and 4-AP. The DPPH, $ABTS^+$, and superoxide scavenging activities of 4-AP-βCD were 2.05-, 1.69-, and 2.99-fold higher than those of 4-AP, respectively

(Fig. 7). While 4-AP-αCD also showed satisfactory results, exhibiting a 1.73-, 1.29-, and 2.41-fold higher DPPH, $ABTS^{+}$, and superoxide scavenging activity, respectively, in comparison to 4-AP.

3.6 In-Vitro Antimicrobial Activity Assay

Similarly, 4-AP, 4-AP-αCD, and 4-AP-βCD exhibited antimicrobial activity against the applied bacterial strains. Out of them, 4-AP-βCD showed a higher inhibition zone, followed by 4-AP-αCD and 4-AP, respectively [Figure 8(a-e)]. In Gram-positive bacteria, the inhibition zone was more prominent than in Gram-negative bacteria.

3.7 In-Vitro Release Study:

The in vitro release behavior of 4-aminopyridine (4-AP) from its inclusion complexes with α- and β-cyclodextrin was systematically evaluated under physiological conditions (37°C, pH 7.4) using a Franz diffusion cell (Fig. 9). Both systems exhibited biphasic release profiles, comprising an initial burst followed by a sustained diffusion phase, attributed to the rapid desorption of surface-associated drug and to the subsequent controlled release of the encapsulated fraction.

Kinetic analysis using the Korsmeyer–Peppas model demonstrated excellent fitting for both complexes, confirming diffusion-controlled release. The 4-AP–α-CD complex showed a higher release rate constant (K = 0.33752) and diffusional exponent (n = 0.0712) with strong linearity (R^2 = 0.9562), whereas the 4-AP–β-CD complex exhibited a significantly lower release rate constant (K = 0.2594), lower diffusional exponent (n = 0.017) and slightly reduced correlation (R^2 = 0.9263), indicating more restricted diffusion (Table 2).In both cases, n < 0.45 confirms Fickian diffusion as the dominant release mechanism.[27] Notably, the dimensionless ratio ($n_\alpha/n_\beta \approx 4.19$) quantitatively demonstrates that diffusion from the α-CD complex is over four times less constrained than that from the β-CD system.

To establish a thermodynamic basis for this behavior, the Gibbs free energy changes (ΔG) of complex formation were considered. The 4-AP–β-CD complex exhibited a more negative ΔG value (− 4.84) compared to the 4-AP–α-CD complex (− 4.27), confirming stronger host–guest interactions and greater thermodynamic stability in the β-CD system. The difference in free energy ($\Delta\Delta G \approx 0.57$) provides a quantitative measure of this enhanced stability. Correspondingly, the dimensionless ratio ($|\Delta G_\beta|/|\Delta G_\alpha| \approx 1.13$) indicates ~ 13% stronger binding in the β-CD complex.

This thermodynamic advantage directly translates into kinetic behavior. The stronger binding (more negative ΔG and higher K□) in the β-CD complex imposes a greater energetic barrier for drug dissociation, thereby reducing the diffusion rate and resulting in sustained release. Conversely, the relatively less negative ΔG of the α-CD complex reflects weaker inclusion, facilitating easier drug escape and faster diffusion.

Thus, an inverse structure–thermodynamics–kinetics relationship is clearly established: stronger binding affinity (higher K□, more negative ΔG) → greater diffusional constraint → slower drug release.

The structural features of cyclodextrins further support this relationship. The larger cavity of β-cyclodextrin enables deeper inclusion and stronger hydrophobic interactions with 4-AP, while the smaller cavity of α-cyclodextrin limits interaction strength, leading to comparatively rapid release.[28, 29]

From a drug delivery perspective, this distinction is critical. The α-CD complex offers faster and more predictable drug availability, suitable for rapid therapeutic onset, whereas the β-CD complex provides prolonged release, advantageous for maintaining steady plasma levels and minimizing peak-related side effects.

Overall, the combined kinetic, thermodynamic, and dimensionless analyses establish a coherent structure–property–function relationship, demonstrating that modulation of cyclodextrin cavity size and binding energetics provides a rational strategy for tuning drug release profiles in supramolecular delivery systems.

Table 2
Release kinetic parameters for 4-AP after fitting *in vitro* release data to the Korsmeyer-Peppas model.

4-AP + α-CD IC	**K_{kp}**	**R^2**	**N**
	0.3375	**0.95**	**0.071**
4-AP + β-CD IC	0.2594	0.92	0.017

3.8 In vitro cytotoxicity studies:

The in-vitro cytotoxicity of 4-aminopyridine (4-AP), α-cyclodextrin (α-CD), β-cyclodextrin (β-CD), and their corresponding inclusion complexes (α-CD–4-AP and β-CD–4-AP) was evaluated using the MTT assay against the Human lung adenocarcinoma (A549) cell line. Cells were treated with increasing concentrations of the test compounds, and cell viability was assessed to generate dose–response curves (Fig. 10).

(A549) cell line following 48 h exposure to free 4-AP, α-CD, 4AP-α-CD, β-CD and 4AP–β-CD host–guest system, and the standard anticancer drug gemcitabine, as determined by the MTT assay. (b) Nonlinear regression analysis of the corresponding dose–response curves used to determine IC_{50} values. Data are expressed as mean ± SD from three independent experiments (n = 3).

Both native cyclodextrins, α-CD and β-CD, exhibited negligible cytotoxicity over the investigated concentration range, confirming their biocompatibility and indicating that the host molecules do not independently contribute to cell growth inhibition. In contrast, free 4-AP exhibited moderate cytotoxicity, with an IC_{50} of 215.95 µg/mL. Upon inclusion complex formation, an enhancement in cytotoxicity was observed. The α-CD–4-AP complex showed improved activity compared to the free drug, with a reduced IC_{50} value of 184.28 µg/mL. Notably, the β-CD–4-AP system exhibited a significantly greater cytotoxic

effect, with an IC_{50} value of 125.04 μg/mL, indicating a marked improvement in biological efficacy. The observed trend in cytotoxic activity follows the order:

β-CD–4-AP > α-CD–4-AP > free 4-AP

The enhanced cytotoxicity of the inclusion complexes cannot be attributed to the cyclodextrins themselves, as both α-CD and β-CD are essentially non-toxic under the experimental conditions. Therefore, the improvement in activity is attributed to host–guest complexation, which modifies the physicochemical properties of 4-AP.

The superior performance of the β-CD–4-AP complex compared to the α-CD system may be rationalized based on differences in cavity size and host–guest compatibility. The relatively larger cavity of β-CD is expected to facilitate more effective encapsulation of 4-AP, leading to improved stabilization and dispersion of the guest molecule in the biological medium. This enhanced encapsulation likely results in increased effective availability of the drug, thereby contributing to the observed increase in cytotoxic response.

Furthermore, inclusion complexation may influence the interaction of 4-AP with the cellular environment by improving its apparent solubility and reducing aggregation, which can enhance its accessibility to biological targets. The comparatively lower activity of the α-CD–4-AP complex suggests less efficient inclusion, consistent with its smaller cavity size.

Although the β-CD–4-AP system exhibited significantly enhanced cytotoxicity relative to the free drug, no direct studies on cellular uptake or intracellular drug release were performed. Therefore, the observed improvement is attributed primarily to formulation-level effects, such as enhanced solubility and molecular accessibility, rather than confirmed intracellular delivery.

Overall, these results highlight the crucial role of cyclodextrin cavity size and host–guest interactions in modulating the biological performance of inclusion complexes, with β-CD emerging as a more effective carrier for 4-AP compared to α-CD.

3.8 Theoretical study of Host-Guest (4-AP-CD) interaction:

Optimized geometries reveal successful encapsulation of 4-AP within both α-CD and β-CD cavities. However, distinct differences in inclusion behavior are observed.

In the β-CD system, 4-AP is deeply embedded within the hydrophobic cavity, forming multiple directional hydrogen bonds with the hydroxyl groups at the rim. In contrast, α-CD, owing to its smaller cavity size, accommodates 4-AP less efficiently, resulting in comparatively restricted insertion.

Binding energies quantitatively support this structural distinction. The 4-AP–β-CD complex exhibits a significantly stronger interaction (ΔE_ads = − 7.65 eV) compared to the 4-AP–α-CD system (ΔE_ads = − 5.88 eV), indicating superior host–guest affinity in β-CD. This difference arises from greater geometric complementarity and stronger hydrogen-bonding interactions within the larger β-CD cavity.To evaluate

the chemical reactivity of the complex in water, parameters such as global hardness, softness, and electronegativity were calculated and tabulated (Table 3). The high binding affinity of 4-AP for *β*-CD is attributed to significant hydrogen bonding interactions. The geometry of these bonds,for both the complexes, indicated by dashed lines (-------), is presented in Fig. 10.

Table 3: HOMO, LUMO levels, band gap and other global parameters for 4-AP,4-AP-α-CD, and 4-AP- β -CD inclusion complexes in water medium.

HOMO (eV)	**4-AP**	**4-AP-α-CD**	**4-AP-*β*-CD**
	-6.43	**-6.34**	**-6.16**
LUMO (eV)	**-0.59**	**-0.71**	**-0.51**
Δ(LUMO −HOMO) (eV)	**5.83**	**5.63**	**5.65**
μ (eV)	**-3.51**	**-3.53**	**-3.34**
χ (eV)	**3.51**	**3.53**	**3.34**
S (eV)	**0.17**	**0.18**	**0.18**
η (eV)	**2.92**	**2.82**	**2.83**
ω (eV)	**2.11**	**2.21**	**1.97**

Frontier molecular orbital and charge transfer characteristics:

Frontier molecular orbital (FMO) analysis was employed to evaluate the stability of the inclusion complexes.[30] The HOMO–LUMO energy gap serves as a key indicator of kinetic stability, chemical reactivity, and molecular hardness. Global reactivity descriptors were calculated using Koopmans' theorem for closed-shell systems [31, 32], and the obtained values in aqueous phase are summarized in Table 3. The 3D plots of the HOMO and LUMO orbitals computed at the B3LYP/6–31 + G(d) level for both complexes are illustrated in Fig. 11.

The HOMO–LUMO energy gap decreases slightly upon complexation for both systems, indicating a marginal enhancement in chemical reactivity.

For the β-CD complex, the energy gap decreases from 5.83 eV (4-AP) to 5.65 eV, while for α-CD it decreases from 5.73 eV to 5.63 eV. The negative chemical potential (μ) values in both systems confirm thermodynamic stability.

A comparative analysis of global descriptors reveals:

- β-CD complex: lower electronegativity (χ) and electrophilicity (ω), indicating reduced tendency for electron acceptance

- α-CD complex: slightly higher electrophilicity, suggesting relatively stronger electron-accepting character
- Despite these variations, the spatial distribution of HOMO and LUMO orbitals in both complexes remains largely localized on the 4-AP molecule, indicating

minimal charge transfer between host and guest. Thus, stabilization is dominated by non-covalent interactions rather than electronic delocalization.

MESP maps highlight the nature of electrostatic interactions within the complexes. Molecular electrostatic potential (ESP) maps were generated to elucidate the nature of host–guest interactions within the complex, as depicted in Fig. 12.

The β-CD system shows prominent regions of negative potential (red zones), indicating strong electrostatic interactions between 4-AP and the cyclodextrin cavity. In contrast, the α-CD complex displays less intense electrostatic features, suggesting comparatively weaker interactions.

Reduced density gradient (RDG) analysis [33] was carried out to examine the non-covalent interactions within the 4-AP-*α*-CD & 4-AP–β-CD host–guest complexes (Fig. 13). RDG analysis provides deeper insight into weak interactions governing stability. The β-CD complex exhibits pronounced red and blue regions corresponding to hydrogen bonding and van der Waals interactions, respectively, confirming multi-modal stabilization. Conversely, the α-CD system shows a relatively smaller contribution from hydrogen bonding and a dominant presence of van der Waals interactions, indicating weaker and less directional binding.

Thus the combined computational results clearly establish that:

- β-CD forms a more stable and energetically favorable inclusion complex with 4-AP than α-CD
- The enhanced stability arises from better cavity size compatibility, deeper encapsulation, and stronger hydrogen bonding networks
- Both systems exhibit minimal charge transfer, confirming that stabilization is primarily governed by non-covalent interactions.

Overall, the DFT investigation demonstrates that while both α-CD and β-CD are capable of forming inclusion complexes with 4-AP, β-CD provides a significantly more favorable host environment. The superior binding affinity, stronger hydrogen bonding interactions, and enhanced electrostatic stabilization make β-CD a more effective carrier for 4-AP. These theoretical findings are in excellent agreement with experimental observations, validating the reliability of the computational approach

Conclusion

This study provides a comprehensive demonstration of cavity size–dependent modulation of host–guest interactions between 4-aminopyridine (4-AP) and cyclodextrins. Comparative analysis of α-

cyclodextrin and β-cyclodextrin systems establishes that subtle variation in cavity dimension critically governs binding affinity, inclusion geometry, and overall functional performance. Spectroscopic investigations (^1H NMR, UV–visible, and FT-IR) confirmed the formation of stable 1:1 inclusion complexes, with significantly larger upfield shifts and spectral perturbations in the β-CD system, indicating deeper penetration and stronger host–guest interactions relative to α-CD.

Quantitative binding analysis revealed a substantially higher association constant for the β-CD complex, accompanied by more negative Gibbs free energy, confirming enhanced thermodynamic stability. These experimental findings were strongly supported by DFT calculations, which demonstrated deeper encapsulation, higher binding energy, and more extensive hydrogen bonding networks in the β-CD system. RDG and MESP analyses further established that stabilization is predominantly governed by van der Waals and hydrogen bonding interactions, with minimal charge transfer contribution.

Importantly, the differences in binding energetics translated directly into functional outcomes. In vitro release studies revealed a clear inverse relationship between thermodynamic stability and release rate, where the β-CD complex exhibited slower, sustained drug release due to stronger binding, while the α-CD complex showed comparatively faster diffusion. Biological evaluations further demonstrated that inclusion complexation enhances functional activity, with the β-CD complex showing superior antioxidant, antimicrobial, and cytotoxic performance compared to α-CD and free 4-AP. These enhancements are attributed to improved molecular dispersion, stabilization, and controlled release behavior imparted by host–guest interactions.

Overall, this work establishes a direct structure–thermodynamics–function relationship, demonstrating that cyclodextrin cavity size can be strategically tuned to control binding strength, release kinetics, and biological efficacy. The findings provide a rational framework for the design of cyclodextrin-based supramolecular drug delivery systems, with β-cyclodextrin emerging as a more effective carrier for optimizing the performance of 4-aminopyridine

Declarations

Declaration of Competing Interest

The authors declare that they have no known competing financial interests or personal relationships that could have appeared to influence the work reported in this paper.

ASSOCIATED CONTENT

Comprehensive elucidations regarding the utilized chemicals, a tabular representation of Job's plot, data showing the association constants, and 1H-NMR spectra capturing the inclusion complexes, and biological activities assay values were provided in meticulous detail.

Credit author statement

***Koushik Baul**: Conceptualization, Formal analysis, Methodology, Investigation, Writing-original draft preparation, Software, Data curation.*

***Priyanka Roy**: Methodology, Data Curation.*

***Subhankar Choudhury**: Software, Data Curation.*

***Biswanath Karmakar:** Formal analysis, Investigation.*

Dibakar Ghosh: Investigation, *Experiment*

***Swarnendu Roy:** Visualization, Investigation.*

***Sangita Dey**: Formal Analysis. Investigation.*

***Anoop Kumar**: Formal Investigation*

***Saurav Sarkar**: physical experimentation, Formal Analysis*

***Gouranga Nandi**: Investigation, Visualization*

***Mahendra Nath Roy**: Supervision.*

Declaration of Competing Interest

The authors declare no competing financial interest

Clinical trial number

Not Applicable

Acknowledgments :

K. Baul thank the Department of Chemistry at the University of North Bengal for their financial and instrumental support. Prof. M.N. Roy, the corresponding author, is deeply appreciative of the one-time Basic Scientific Research (BSR) grant from the University Grants Commission (UGC) in New Delhi, India. This non-recurring endowment, provided through Grant-in-Aid No. F.4-10/2010 (BSR), acknowledges his dedicated contributions to scientific research and supports the continuation of his investigations. Additionally, Prof. M.N. Roy is grateful to the UGC for the instrumental facilities provided under reference No. RP/5032/FCS/2011, New Delhi, which has been crucial for his ongoing project. The authors also acknowledge the Department of Botany, Department of Bio-technology, and Department of Pharmaceutical Technology, University of North Bengal, Darjeeling, India, for their analytical and instrumental support, as well as CDRI-SAIF, Lucknow, for providing the analytical instrumentation facilities, including FTIR and 1H NMR measurements.

Ethical Approval

Not Applicable.

Funding

1. Basic Scientific Research (BSR),Grant-in-Aid No. F.4-10/2010 (BSR), from the University Grants Commission (UGC) in New Delhi, India.

2. Grant from the University Grants Commission (UGC) in New Delhi, India for the instrumental facilities provided under reference No. RP/5032/FCS/2011

Availability of data and materials

The data analysed during the study has available on permission to corresponding author.

References

1. Horton, L., Conger, A., Conger, D., Remington, G., Frohman, T., Frohman, E., Greenberg, B.: Effect of 4-aminopyridine on vision in multiple sclerosis patients with optic neuropathy. Neurology. **80**(20), 1862–1866 (2013)
2. Sarah, A., Morrow, H., Rosehart, A.M., Johnson: The effect of Fampridine-SR on cognitive fatigue in a randomized double-blind crossover trial in patients with MS. Mult Scler. Relat. Disord. **11**, 4–9 (2017)
3. Sarah, D., Broicher, L., Filli, O., Geisseler, N., Germann, B., Z¨orner, P., Brugger, M., Linnebank: Positive effects of fampridine on cognition, fatigue and depression in patients with multiple sclerosis over 2 years. J. Neurol. **265**, 1016–1025 (2018)
4. Hayes, K.C., Blight, A.R., Potter, P.J., Allatt, R.D., Hsieh, J.T.C., Wolfe, D.L., Lam, S.: Hamilton, Preclinical trial of 4-aminopyridine in patients with chronic spinal cord injury. Spinal Cord. **31**(4), 216–224 (1993)
5. Leussink, V.I., Montalban, X., Hartung, H.-P.: Restoring axonal function with 4-aminopyridine: clinical efficacy in multiple sclerosis and beyond. CNS Drugs. **32**(7), 637–651 (2018)
6. Szejtli, J.: Introduction and General Overview of Cyclodextrin Chemistry. Chem Rev. ;98(5):1743–1754. (1998). 10.1021/cr970022c. PMID: 11848947
7. Loftsson, T., Duchêne, D.: Cyclodextrins and their pharmaceutical applications. Int. J. Pharm. **329**(1–2), 1–11 (2007). 10.1016/j.ijpharm.2006.10.044 Epub 2006 Nov 9. PMID: 17137734
8. Del Valle, E.M.M.: Cyclodextrins and Their Uses: A Review. Process Biochem. **39**, 1033–1046 (2004)
9. https://doi.org/10.1016/S0032-9592(03)00258-9
10. Brewster, M.E., Loftsson, T.: Cyclodextrins as pharmaceutical solubilizers. Adv Drug Deliv Rev. ;59(7):645 – 66. (2007). 10.1016/j.addr.2007.05.012. Epub 2007 May 29. PMID: 17601630
11. Christoph, A., Schalley: Analytical Methods in Supramolecular Chemistry, 1. Wiley (2012)

12. Priyanka Roy, M., Mondal, A., Hossain, D., Roy, K., Mallick, S., Debnath, M.S., Haydar, S., Dey, S., Sarkar, S., Choudhury, T., Ray, A., Kumar: Gouranga Nandi, Mahendra Nath Roy, Investigation of the host–guest inclusion complex of 4-aminopyridine with α-cyclodextrin: A physicochemical and computational study for biochemical applications. J. Mol. Struct., 1343,2025,142799, ISSN 0022-2860.
13. Simona, J., Dani, D., Petr, S., Marcela, N., Jakub, T., Bohuslava, T.: Edible films from carrageenan/orange essential oil/trehalose—structure, optical properties, and antimicrobial activity. Polymers. **13**(3), 332 (2021)
14. Ilona, M.-G., Villafuerte-Robles, L.: Influence of enteric-coated lactose on the release profile of 4-aminopyridine from HPMC matrix tablets. Pharm. Dev. Technol. **9**(2), 145–153 (2004)
15. Mosmann, T.: Rapid colorimetric assay for cellular growth and survival: application to proliferation and cytotoxicity assays. J. Immunol. Methods. **65**, 55–56 (1983)
16. Dutta, A., Chakraborty, A., Ghosh, T., Kumar, A.: 5-Fluorouracil induces apoptosis in nutritional deprived hepatocellular carcinoma through mitochondrial damage. Sci. Rep. **14**, 23387 (2024)
17. Gaussian, C., Frisch, M.J., Trucks, G.W., Schlegel, H.B., Scuseria, G.E., Robb, M.A., Cheeseman, J.R., Scalmani, G., Barone, V., Petersson, G.A., Nakatsuji, H., Fox, D.J., Li, J.-L., Mendeleev, X., Adler, B., Nguyen, M.Q., Byrd, C.M., Gill, P.M., Hay, P.G., Head-Gordon, M., Johnson, B.G., Herbert, M.P., Khoo, L.A., Nguyen, T.V., Replogle, E.S., Brooks, A.P., Collins, J.B., Chen, D.L., Adamo, C., Gomperts, R., Stratmann, R.E., Yazyev, O., Austin, A.J., Cammi, R., Pomelli, C., Ochterski, J.W., Martin, R.L., Morokuma, K., Zakrzewski, V.G., Voth, G.A., Salvador, P., Dannenberg, J.J., Dapprich, S., Daniels, A.D.: (2016). Ö. Farkas, F. Foresman, J. B. Fox, J. E. Gaussian, Inc., Wallingford, CT
18. Deb, M., Roy, S., Hassan, N., Roy, J.S.D., NarendraNath, Ghosh, P.K.C., Maiti, D.K.: and NayanRanjanSingha. Chromo-Fluorogenic Sensing of Fe (III), Cu (II), and Hg (II) Using a Redox-Mediated Macromolecular Ratiometric Sensor. ACS Applied Polymer Materials 5, no. 7 : 4820–4837. (2023)
19. Ghosh, N.N., Habib, M., Pramanik, A., Sarkar, P., Pal, S.: Molecular engineering of anchoring groups for designing efficient triazatruxene-based organic dye-sensitized solar cells. New J. Chem. **43**(17), 6480–6491 (2019)
20. Cossi, M., Barone, V., Cammi, R., Tomasi, J.: Ab initio study of solvated molecules: a new implementation of the polarizable continuum model. Chem. Phys. Lett. **255**, 327–335 (1996)
21. Lu, T., Chen, F.: Multiwfn: a multifunctional wavefunction analyzer. J. Comput. Chem. **33**(5), 580–592 (2012)
22. Mondal, M., Basak, S., Choudhury, S., Ghosh, N.N.: Roy,Investigation of molecular interactions insight into some biologically active amino acids and aqueous solutions of an anti-malarial drug by physicochemical and theoretical approach. J. Mol. Liq. **341**, 116933 (2021)
23. Deb Roy, J., Sankar, M., Deb, M.D., HussainSanfui, S., Roy, A., Dutta: PijushKantiChattopadhyay, NarendraNath Ghosh, Subhasis Roy, and NayanRanjanSingha. Light-Emitting Redox Polymers for

Sensing and Removal-Reduction of Cu (II): Roles of Hydrogen Bonding in Nonconventional Fluorescence. ACS Appl. Polym. Mater. **4**(3), 1643–1656 (2022)

24. Benesi, H.A., Hildebrand, J.H.: A Spectrophotometric Investigation of the Interaction of Iodine with Aromatic Hydrocarbons. J. Am. Chem. Soc. **71**, 2703–2707 (1949)
25. Koushik Baul, P., Roy, D., Roy, S., Choudhury, B., Karmakar, S., Roy, S., Dey, A., Kumar: Tanusree Ray, Mahendra Nath Roy,Exploring host–guest complexation of 5-Fluoro-2'-deoxyuridine with β-cyclodextrin: Spectroscopic and computational insights with anticancer relevance. J. Mol. Struct. Volume **1357**,2026,145252,ISSN 0022–2860
26. Koushik Baul, N., Roy, S., Deb, S., Choudhury, B., Ghosh, D., Roy, B., Karmakar, M.M., Sarkar, S., Roy: Prof.(Dr.) Mahendra Nath Roy.Enhancement of Solubility and Bioactivity of Zonisamide Through Supramolecular Inclusion With β-Cyclodextrin: A Comprehensive Analytical and Computational Study, chemistryselect Volume10, Issue4,January 28, 2025,e202405413
27. Niloy Roy, P., Bomzan, D., Roy, B., Ghosh, M.N., Roy: Exploring β-CD grafted GO nanocomposites with an encapsulated fluorescent dye duly optimized by molecular docking for better applications. J. Mol. Liq. **329**, 115481 (2021)
28. Ritger, P.L., Peppas, N.A.: A simple equation for description of solute release I. Fickian and non-fickian release from non-swellable devices in the form of slabs, spheres, cylinders or discs. J. Controlled Release. **5**(1), 23–36 (1987)
29. Del Valle, E.M.: Cyclodextrins and their uses: a review. Process Biochem. **39**(9), 1033–1046 (2004)
30. Saokham, P., Muankaew, C., Jansook, P., Loftsson, T.: Solubility of cyclodextrins and drug/cyclodextrin complexes. Molecules. **23**(5), 1161 (2018)
31. Koushik Baul, P., Roy, D., Roy, S., Choudhury, B., Karmakar, S., Roy, S., Dey, A., Kumar: Tanusree Ray, Mahendra Nath Roy,Exploring host–guest complexation of 5-Fluoro-2'-deoxyuridine with β-cyclodextrin: Spectroscopic and computational insights with anticancer relevance. J. Mol. Struct., 1357,2026,145252, ISSN 0022-2860
32. Tsuneda, T., Song, J.W., Suzuki, S., Hirao, K.: On Koopmans' theorem in density functional theory. The Journal of chemical physics, 133(17). (2010)
33. Maiti, R., Ghosh, N.N., Khan, A.A., Baildya, N., Maiti, D.K.: Comparative study of CO2 activation on alkali metals encapsulated III–V hollow nanocages: An insight from first-principles calculations. Phys. Lett. A. **412**, 127554 (2021)
34. Contreras-García, J., Johnson, E.R., Keinan, S., Chaudret, R., Piquemal, J.-P., Beratan, D.N., Yang, W.: NCIPLOT: a program for plotting noncovalent interaction regions. J. chem. theory comput. **7**(3), 625–632 (2011)

Scheme

Scheme 1 is available in the Supplementary Files section.

Figures

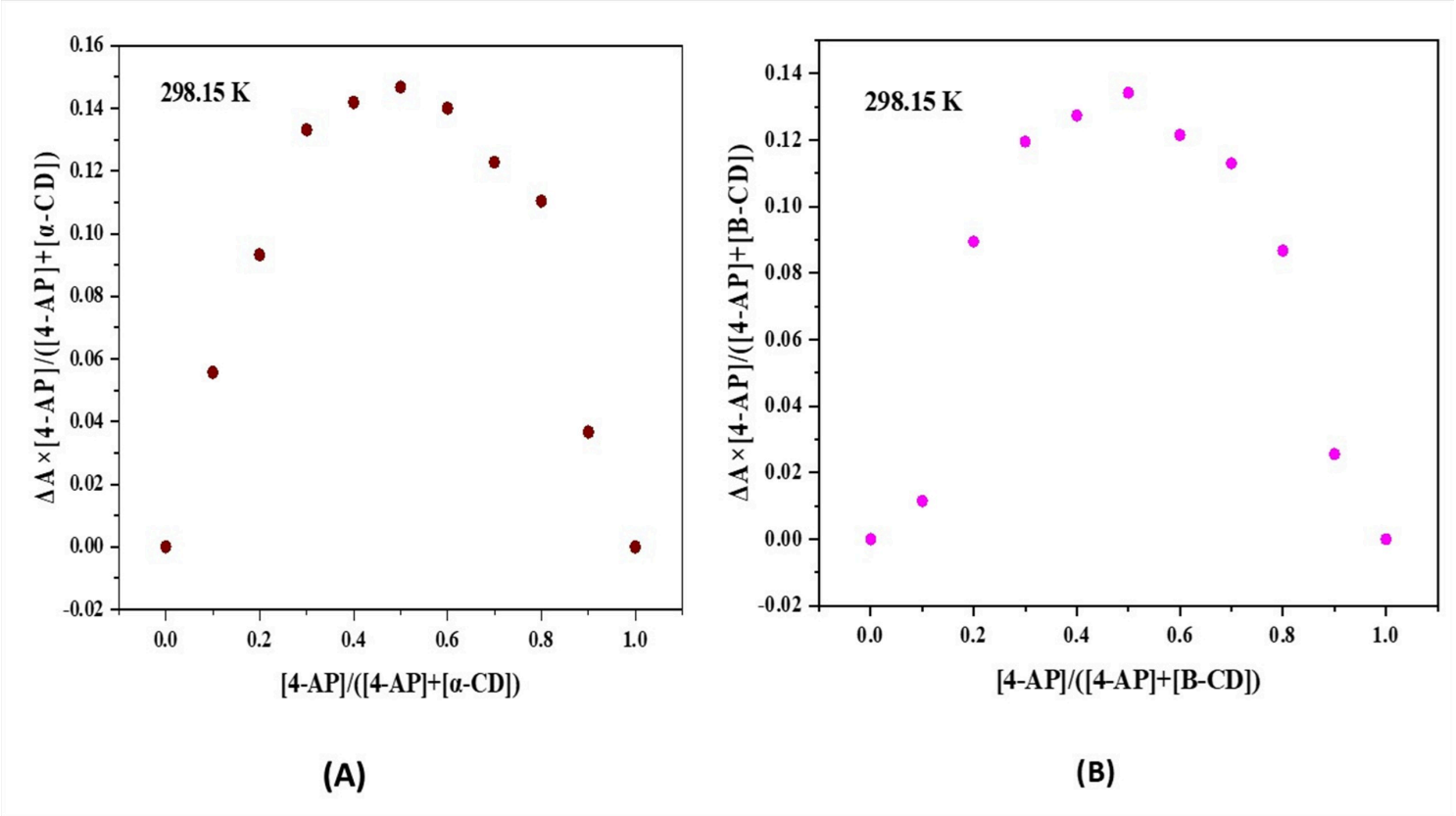


Figure 1

Job's Plot of the (a) 4-AP+α-CD and (b) 4-AP+β-CD system at 298.15 K.

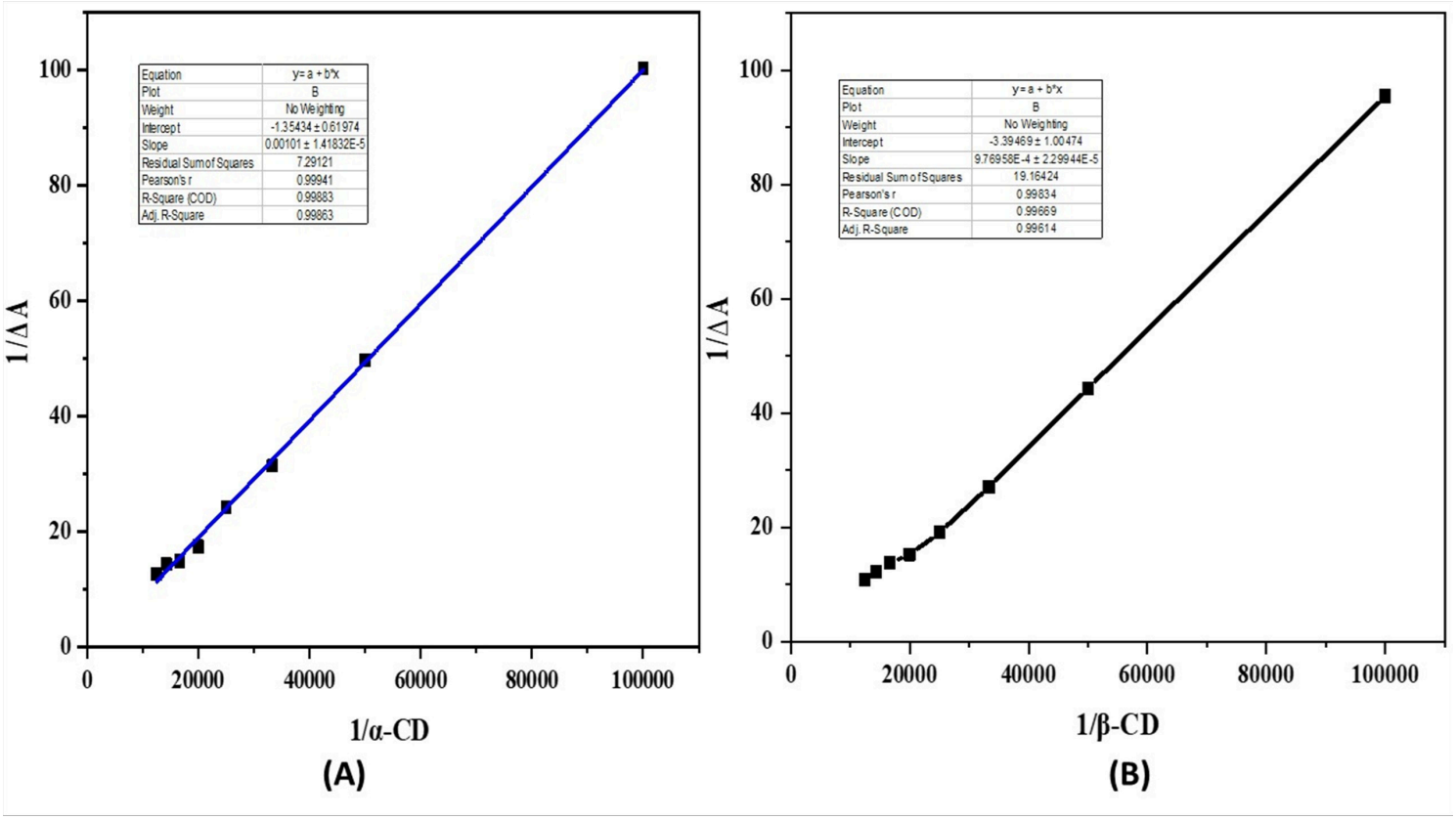


Figure 2

Benesi-Hildebrand double reciprocal plot for the effect of *α*-CD (A) and β-CD (B) on the absorbance of 4-AP (263 nm) at 298.15 K

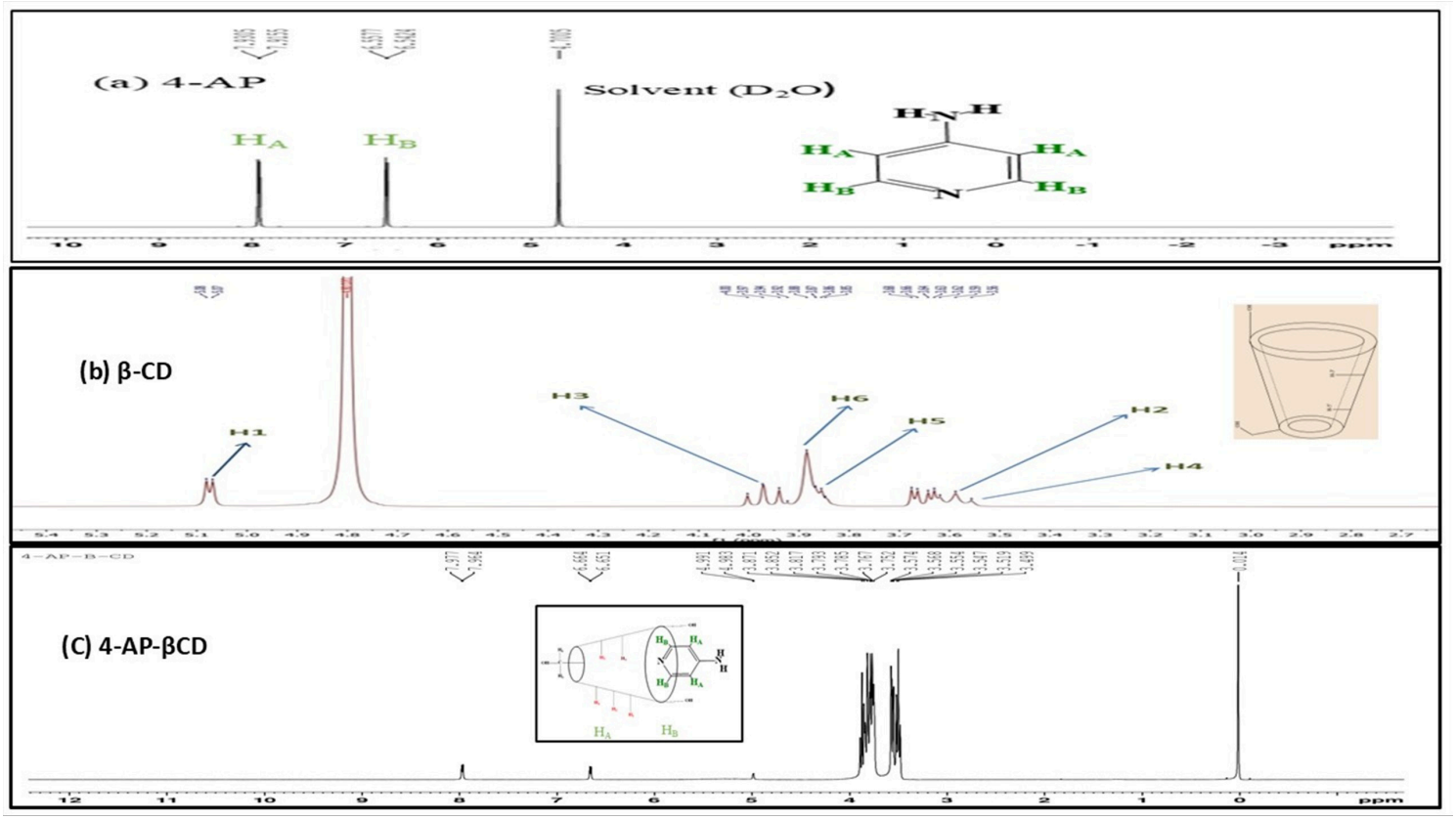


Figure 3

^{1}H NMR spectra of pure (a) 4-AP , (b) β-CD and (c) 4-AP-β-CD IC in D_2O at 298.15 K.

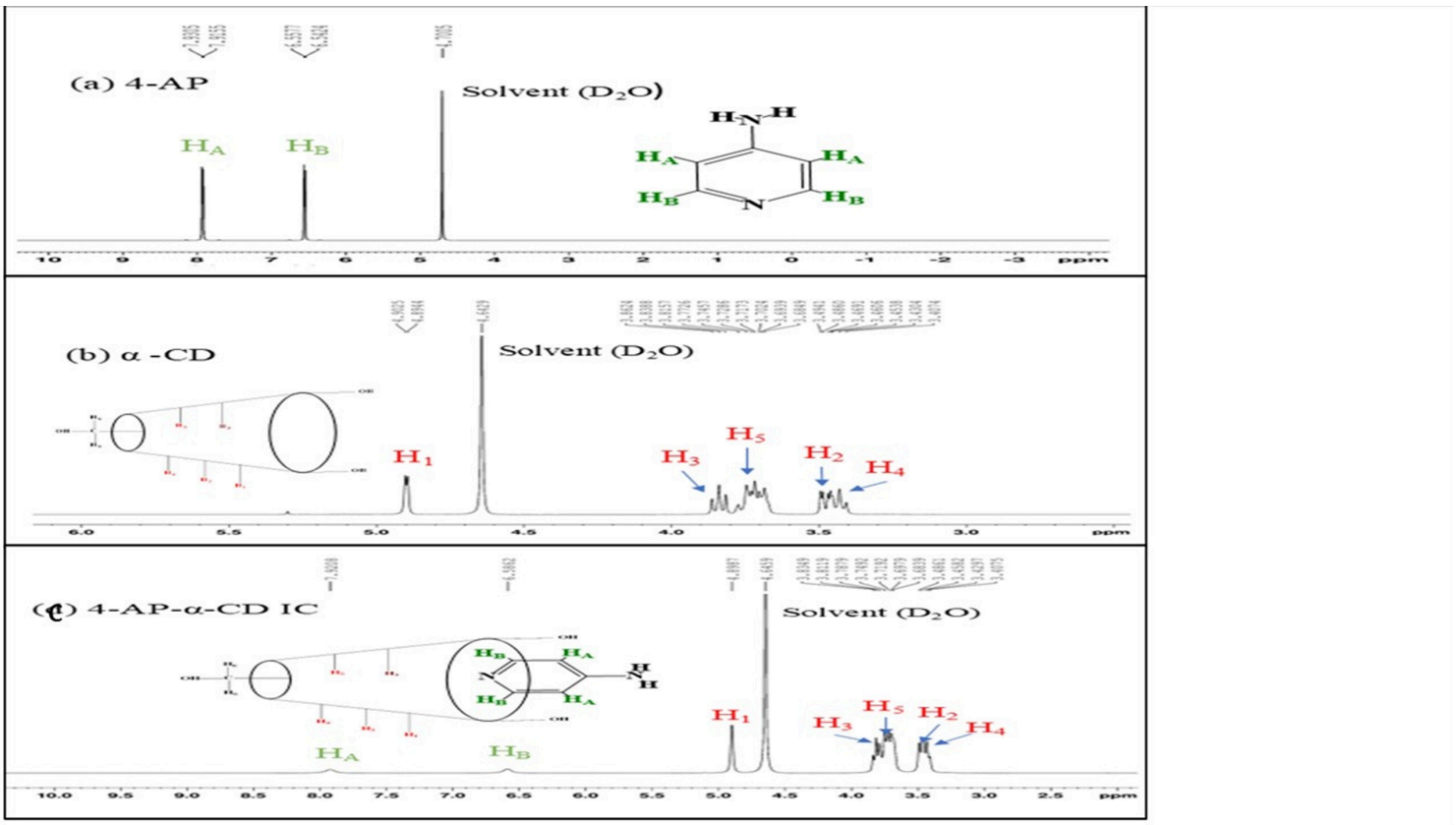


Figure 4

^{1}H NMR spectra of pure (a) 4-AP , (b) α -CD and (c) 4-AP+α-CD IC in D_2O at 298.15 K.

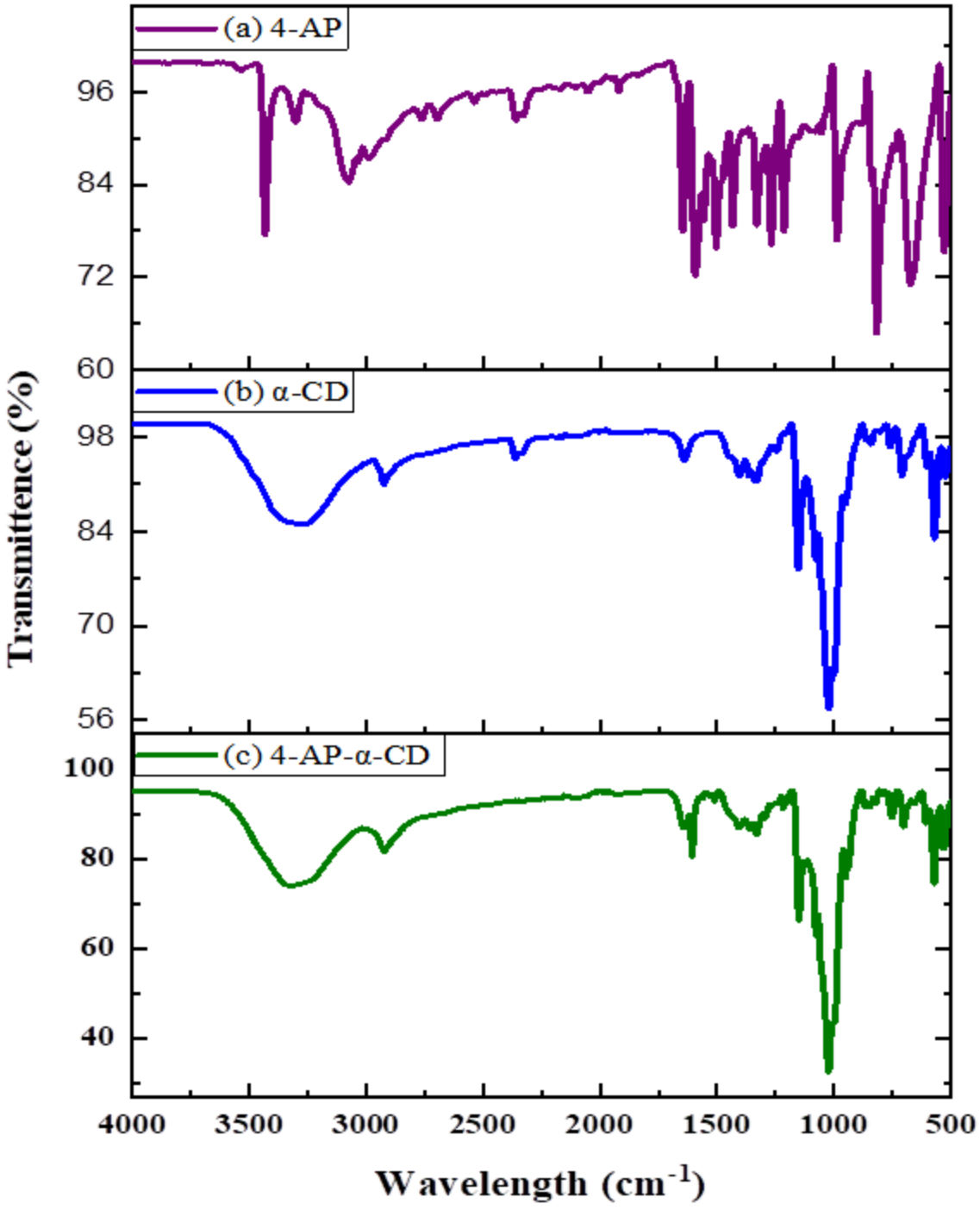


Figure 5

IR Spectra of Pure 4-AP (a), α-CD (b), and 4-AP-α-CD IC (c)

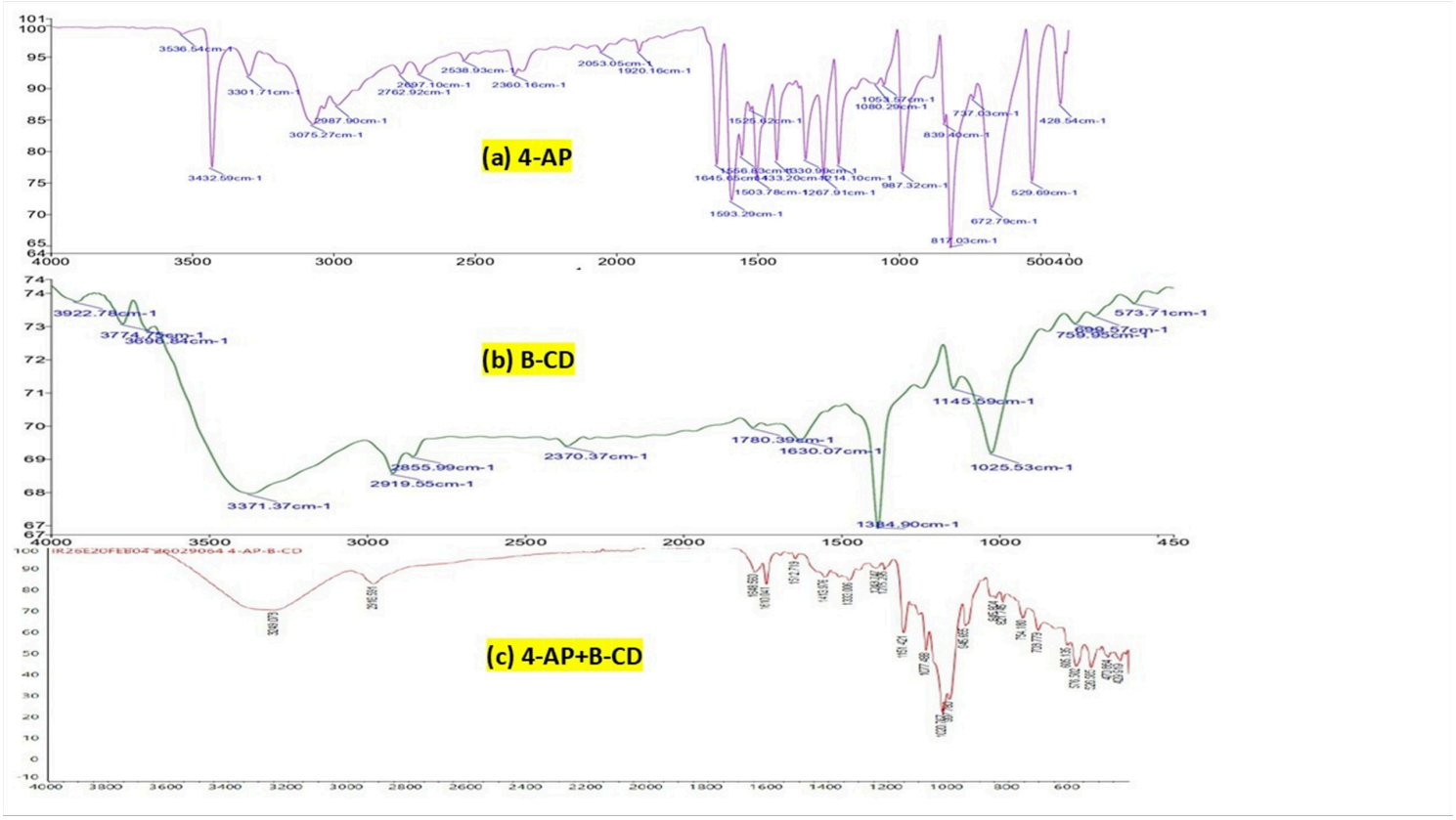


Figure 6

IR Spectra of Pure 4-AP (a), β-CD (b), and 4-AP-β-CD IC (c)

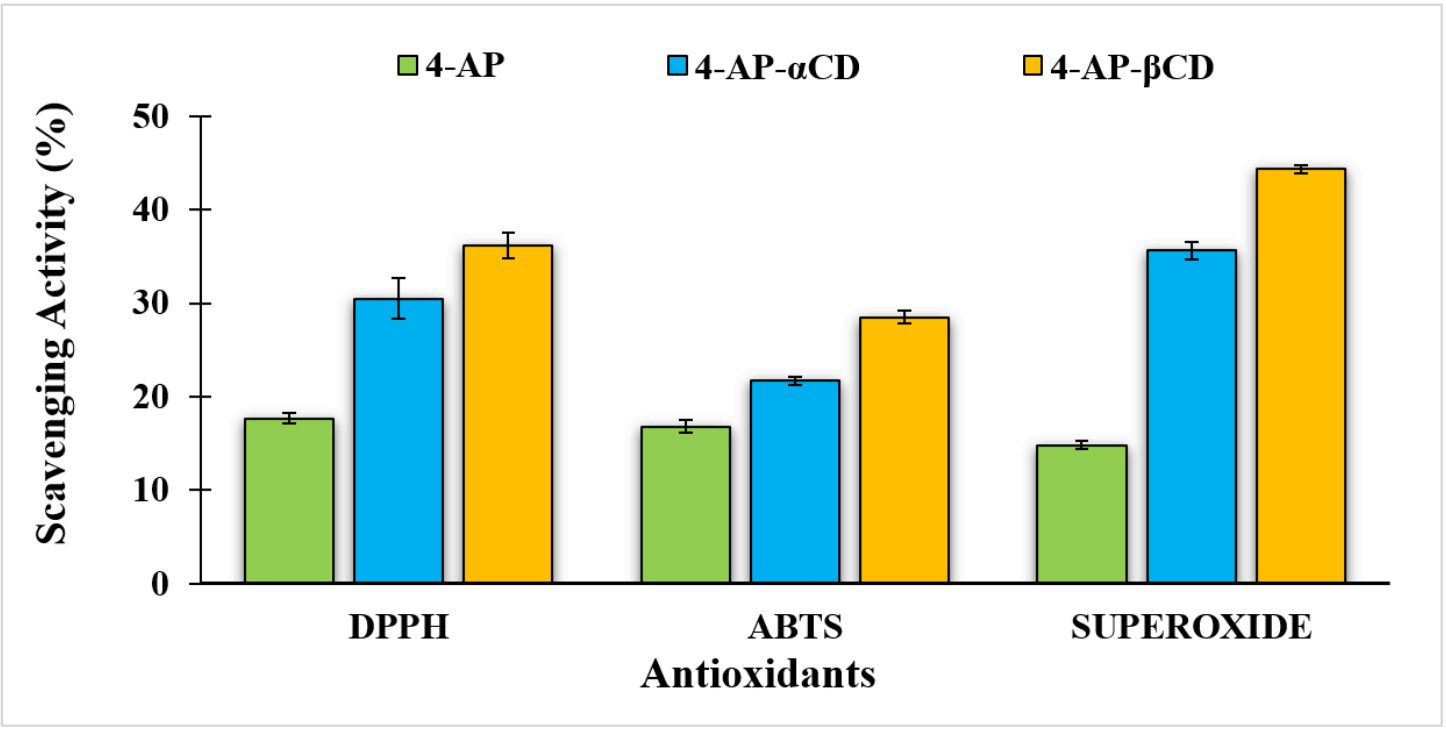


Figure 7

Plot of Scavenging vs free radical

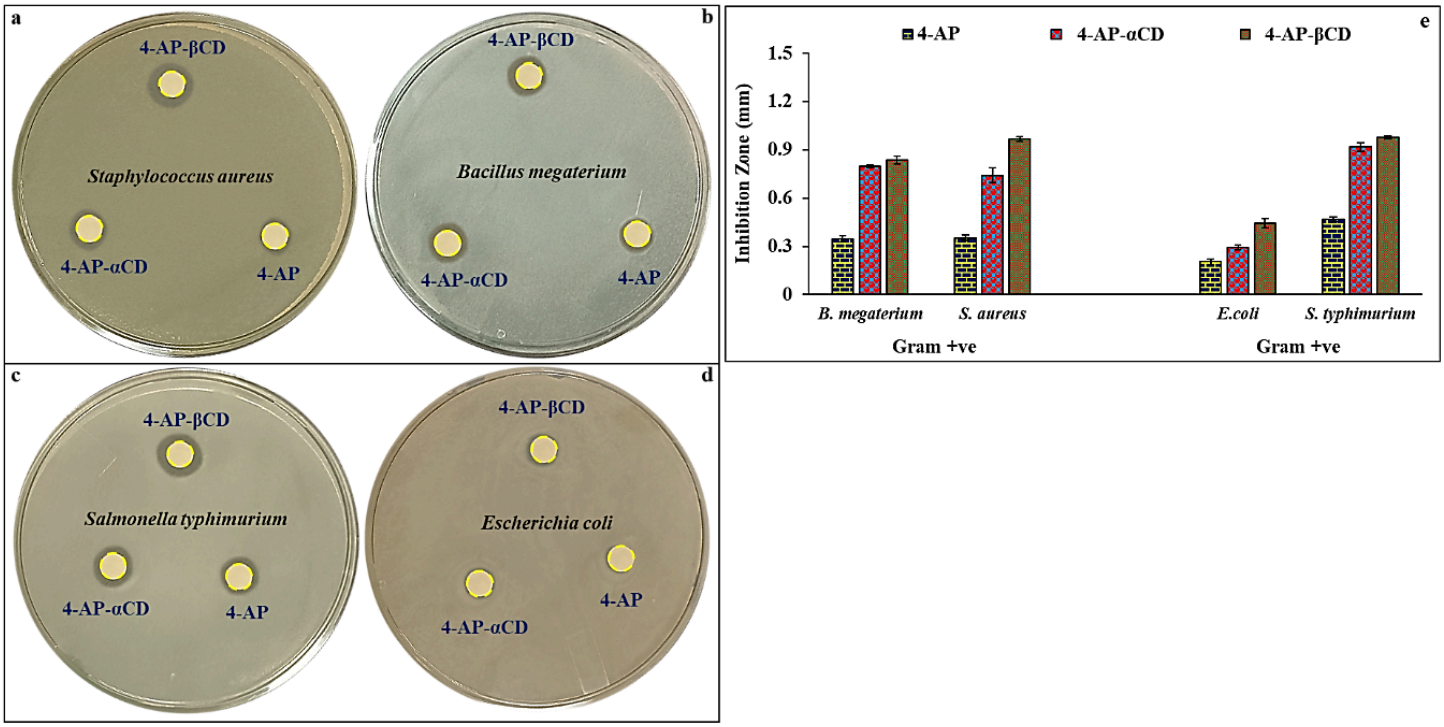


Figure 8

Antimicrobial activity of the biofilm samples against the selected gram-positive and gram negative bacteria (a) *Staphylococcus aureus, (b) Bacillus megaterium (c) Salmonella typhimurium (d) Escherichia coli.*

(*e) Graphical representation of the inhibition zone of the biofilm samples against all the bacteria*

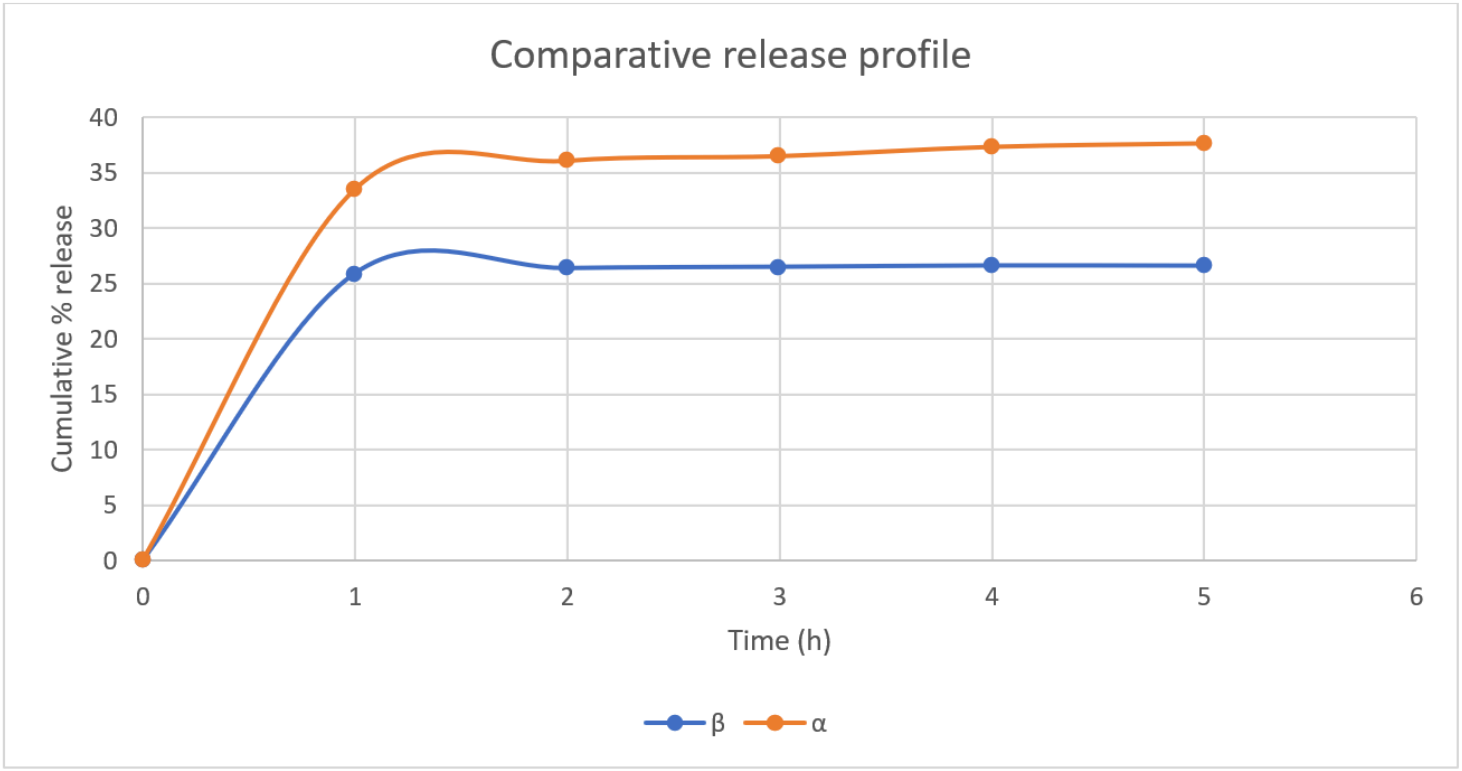


Figure 9

Release profile of 4-AP-α-CD IC and 4-AP-β-CD (1:1 mole ratio). The profile matches the Korsmeyer-Peppas model, as the solid lines indicate

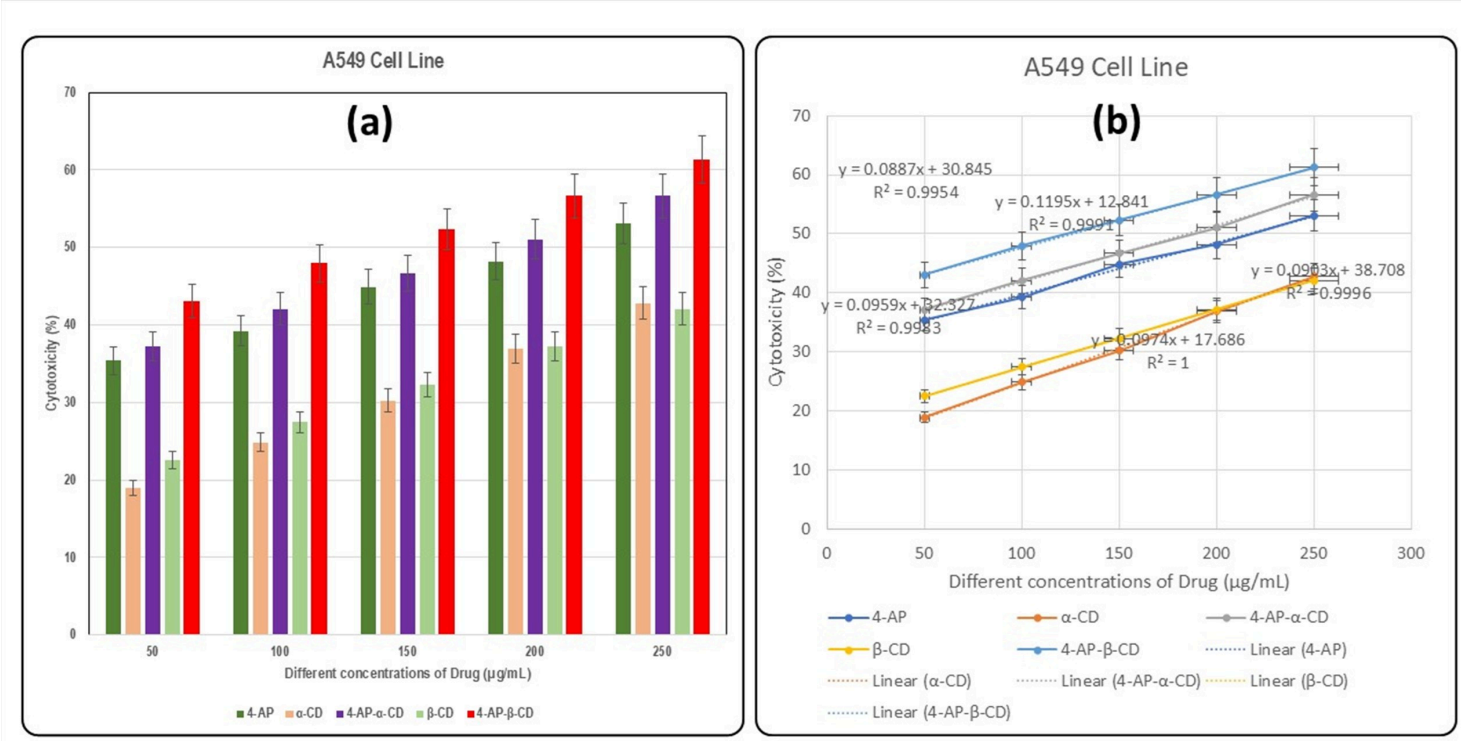


Figure 10

(a) Dose-dependent growth inhibition of the human non-small cell lung cancer (A549) cell line following 48 h exposure to free 4-AP, α-CD, 4AP-α-CD, β-CD and 4AP–β-CD host–guest system, and the standard anticancer drug gemcitabine, as determined by the MTT assay. (b) Nonlinear regression analysis of the corresponding dose–response curves used to determine IC_{50} values. Data are expressed as mean ± SD from three independent experiments (n = 3).

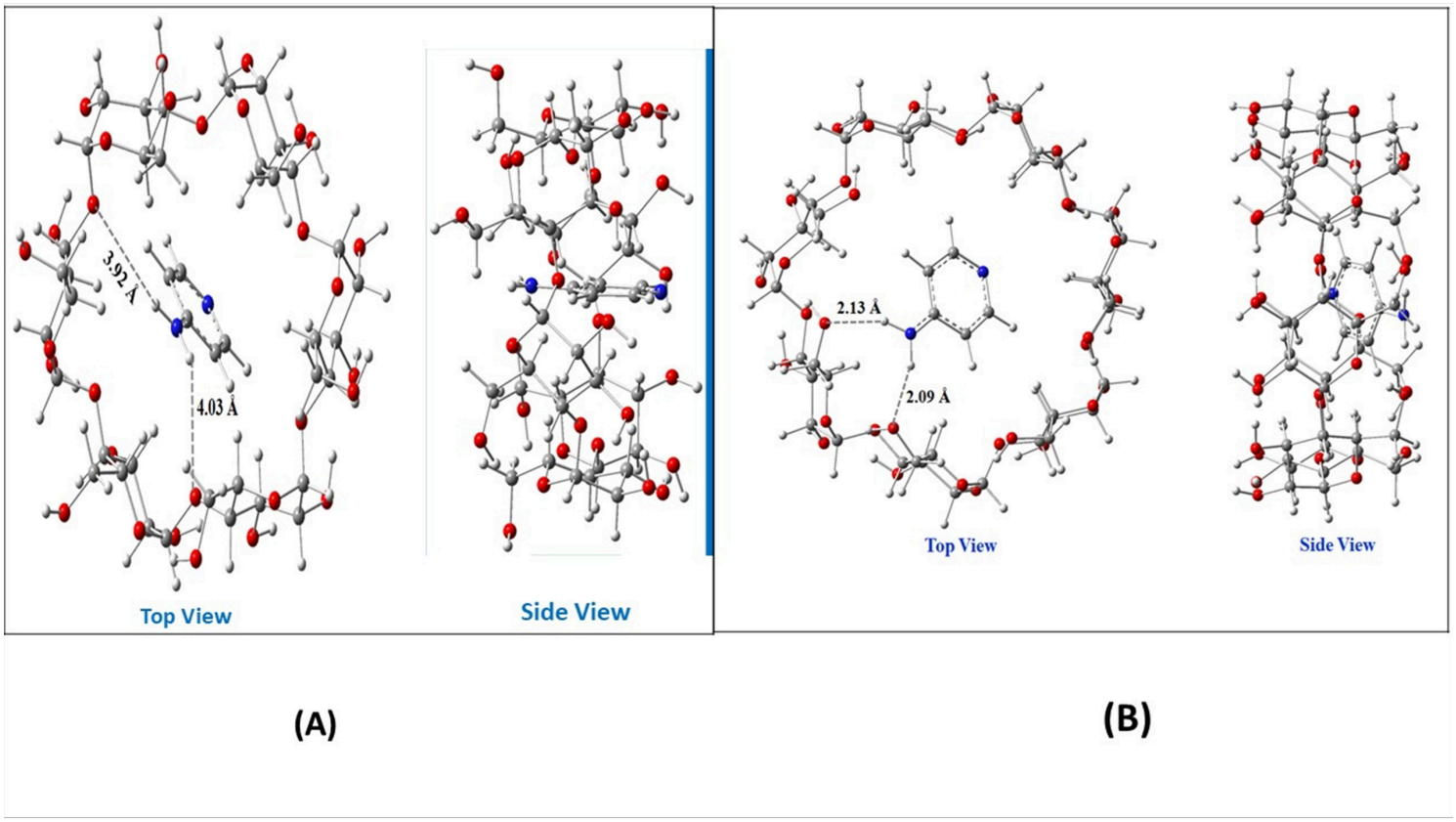


Figure 11

Geometry optimization of the molecules at B3LYP/6-31+G(d) level of theory. Top and side views of the **(A)** 4-AP-*β*-CD & **(B)** 4-AP-*β*-CD.

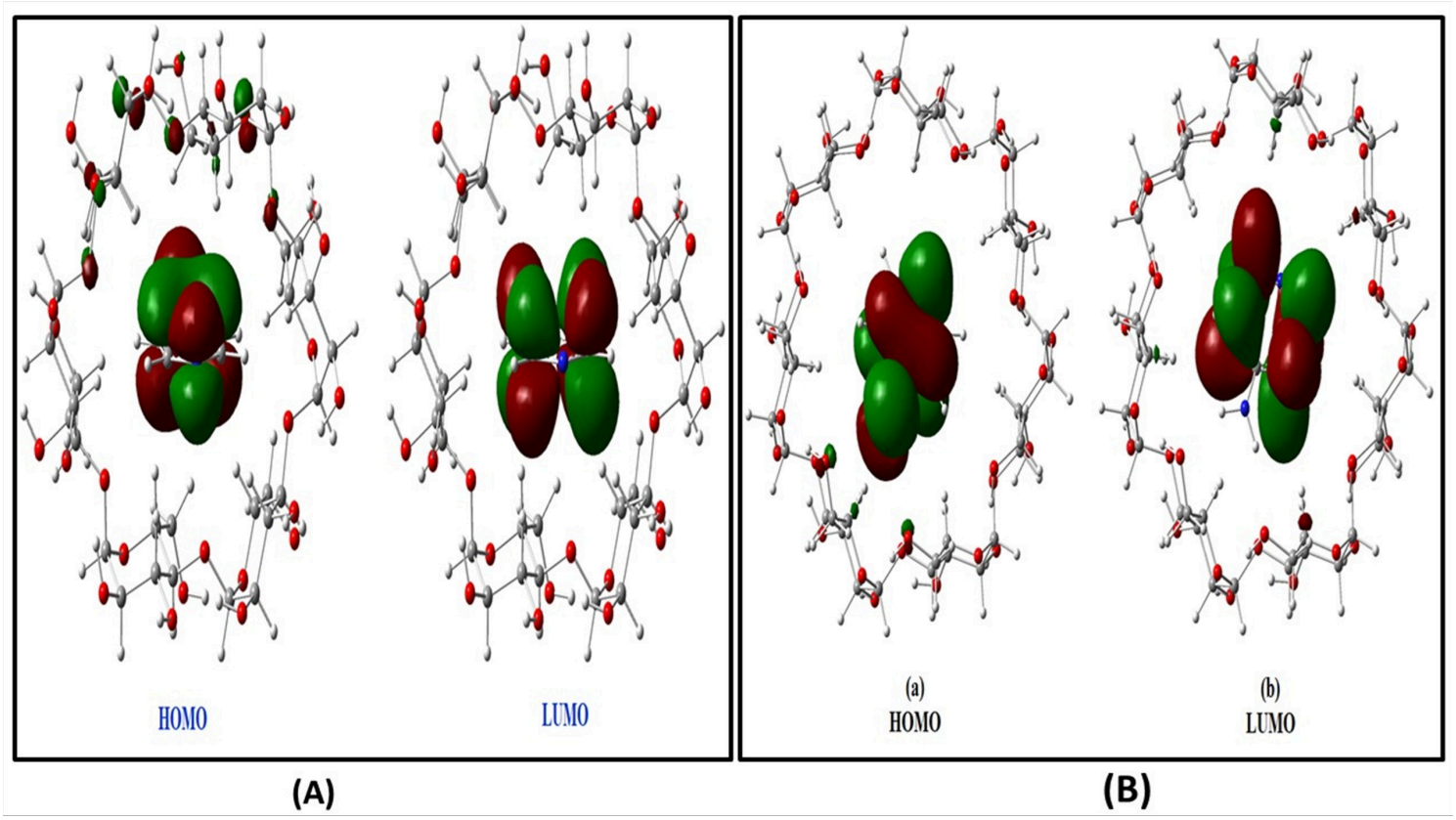


Figure 12

HOMO and LUMO charge densities of **(A)** 4-AP-*β*-CD & **(B)** 4-AP-*β*-CD inclusion complex

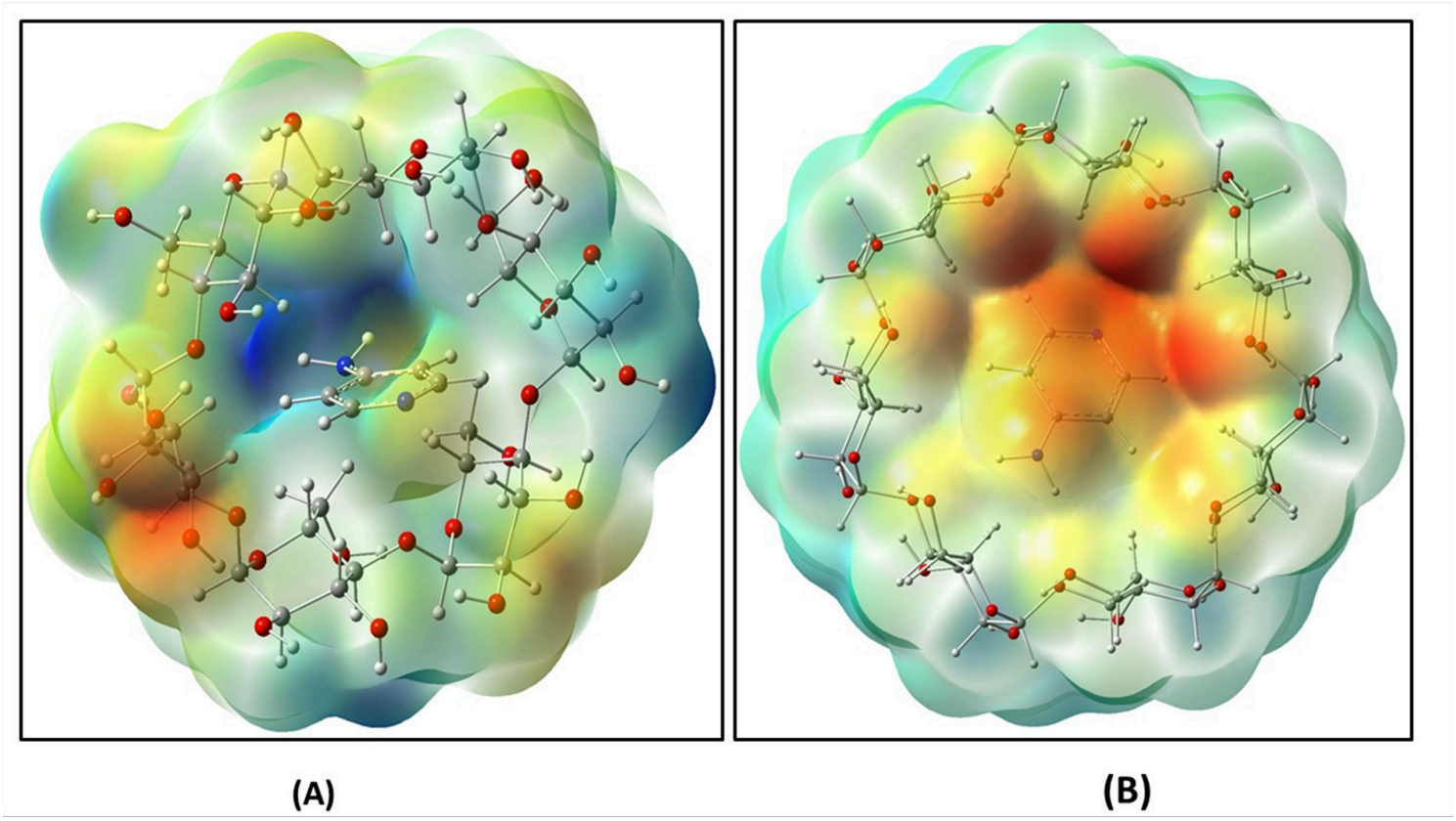


Figure 13

Electrostatic potential map for **(A)** 4-AP-*α*-CD & **(B)** 4-AP-*β*-CD inclusion complexes.

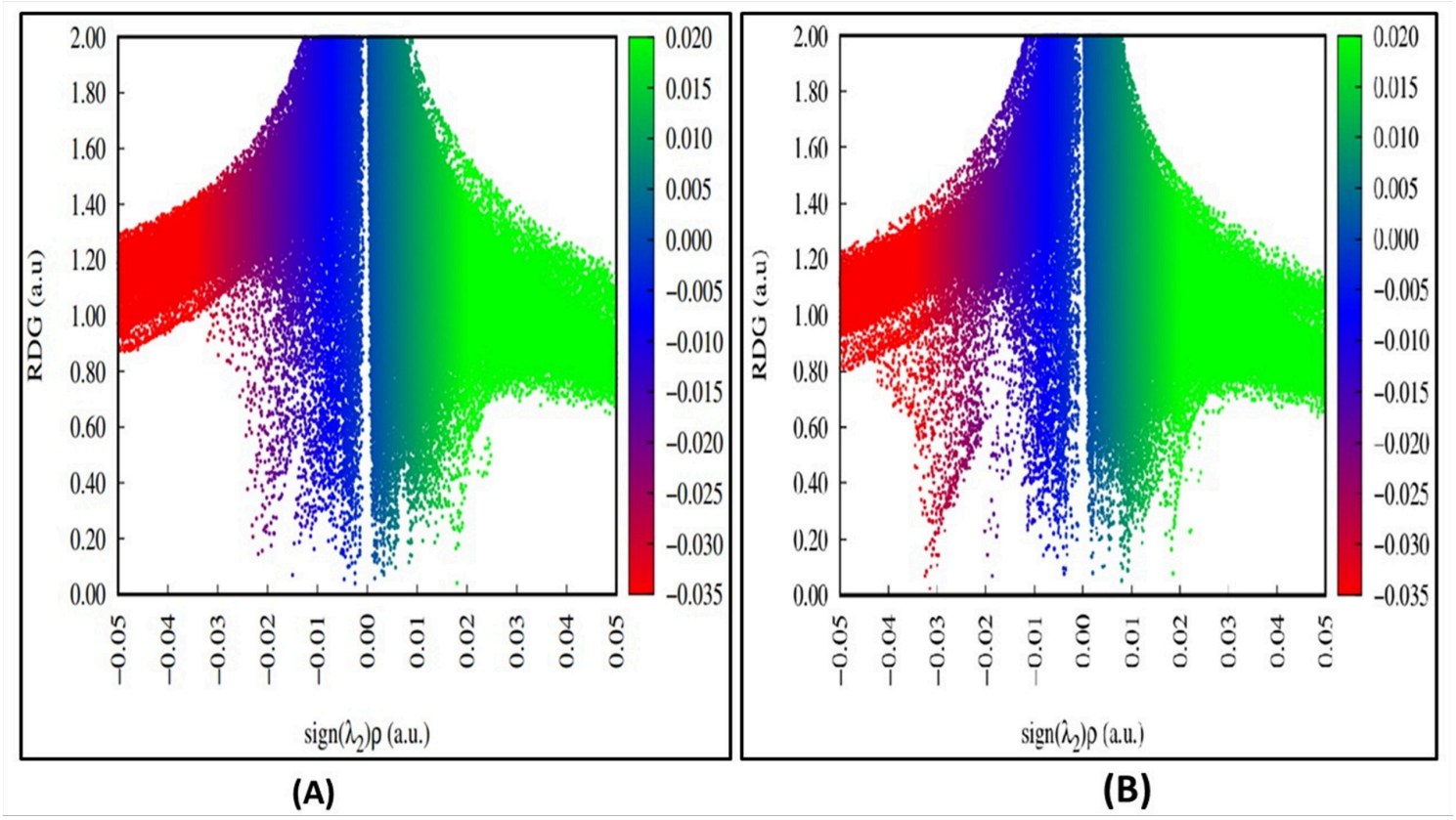


Figure 14

Plots of reduced density gradient (RDG) for **(A)** 4-AP-*α*-CD & **(B)** 4-AP-*β*-CD inclusion complexes.

Supplementary Files

This is a list of supplementary files associated with this preprint. Click to download.

- scheme.png
- SUPPORTINGINFOKOUSHIK.docx